A Systematic Density Functional Theory Study of $V_xO_y^+$ and V_xO_Y (X = 2−4, Y = 2−10) Systems

Mònica Calatayud, Juan Andrés,* and Armando Beltrán

Departament de Ciències Experimentals, Universitat Jaume I, P.O. Box 224, E−12080 Castelló, Spain

Received: April 23, 2001; In Final Form: July 24, 2001

A theoretical study on geometrical, thermodynamic and electronic properties of $V_xO_y^+$ and V_xO_y ($x = 2-4$, $y = 2-10$) systems in different electronic states has been carried out. Analytical gradient techniques with a hybrid spin unrestricted and spin restricted Hartree−Fock density functional method (B3LYP) have been used. An analysis of potential energy surfaces at ground and some excited states renders the most stable structures an their corresponding vibrational frequencies. The reaction energies of the possible decomposition channels are reported and the results indicate that the formation of larger clusters is energetically favorable from the smaller VO^+ ($^3\Sigma$), VO ($^4\Sigma$), VO_2 ($^2A_1$), VO_3 ($^2A'$),V_2O_4 ($^3A''$) and V_2O_5 ($^1A'$) systems and O_2 ($^3\Sigma_g$). A comparative discussion of the bonding in these species has been carried out on the basis of the topological analysis of the electron localization function. Numerical results are analyzed and confronted with available experimental data.

1. Introduction

Small clusters formed by transition metal oxides are of large importance in technical, chemical, and physical research and therefore constitute frequently studied systems, exhibiting a wide variety of structures and properties.[1,2] These clusters are the building blocks for developing cluster-assembled materials and most effort is evidently put because of the important technological applications.[3−7] Interest in the nature of metal−oxygen bonds is justified because there is a close relationship between their structural, physical, and chemical properties whose study can provide a proper rationalization of their behavior at an atomic scale. Depending on the metal-to-oxygen content, the transition metal oxides are characterized by different metal−oxygen bonding and a wide range of behavior is observed.

Metal oxide clusters provide a considerable challenge to state-of-the-art experimental and theoretical techniques. Much progress in this field has been made with the aid of beam techniques, which allow the synthesis and characterization of metal oxides of well-defined size. Recent experiments carried out by Castleman et al.[8−11] have been devoted to study the clusters belonging to the vanadium oxide family; while Bernstein et al.[12] have studied their growth dynamics. These experimental studies open the possibility to carry out a complementary theoretical analysis in order to interplay much closer between theory and experiment in this field.

Quantum chemical calculations offer an alternative to obtain structural parameters, vibrational frequencies, dissociation energies, and the description of the bonding in these systems. As a part of a program directed toward the study of metal oxide clusters using quantum chemical procedures to shed light on the physical/chemical properties,[13−16] the aim of this paper is to complete previous calculations on VO_x^+ and VO_x ($x = 1-4$) systems[17,18] by studying more complex vanadium oxide clusters.

Finally, during the preparation of the present manuscript Vyboishchikov and Sauer[19] have presented a theoretical study from density functional calculations on the ground electronic states of mononuclear, VO_y^- ($y = 1-4$), and binuclear, $V_2O_y^-$ ($x = 4$, 6, and 7), and well as the polynuclear $V_3O_8^-$, $V_4O_{10}^-$ and $V_4O_{11}^-$ anions. In the present work, we have calculated the most stable geometries for each electronic state with different spin multiplicities for both neutral and positively charged vanadium oxides, $V_xO_y^+$ and V_xO_y ($x = 2-4$, $y = 2-10$), within the DFT formalism. A detailed analysis of the potential energy surfaces for each electronic state provides the geometries and the corresponding vibrational properties of these species. The thermodynamic stability of clusters can be studied by analyzing their fragmentation energies. The Electron Localization Function (ELF) is used to obtain the nature of the bonding for the most relevant systems.

The layout of this paper is as follows. The next section is devoted to the description of the computational procedure together with a brief formulation of ELF. In the next section, the results are reported and discussed, first the geometries, energetics and thermodynamic stabilities of different clusters are obtained, followed by the vibrational frequencies analysis and finally a topological analysis of ELF provides a description of the nature of chemical bonding in the most stable clusters. A short section of conclusions closes the paper.

2. Computational Methods

Calculations were performed with GAUSSIAN94 program package.[20] The systems' wave functions have been computed at the restricted HF or unrestricted HF levels, and the 6-31G* basis set developed by Pople et al.[21] has been used. Correlation effects have been introduced by performing spin-polarized DFT calculations using the Becke's three-parameter hybrid nonlocal exchange functional[22] combined with the Lee−Yang−Parr gradient corrected correlation functional,[23] B3LYP. An analysis of the very recent literature shows that DFT methodology renders reliable results and it can be considered a well established theoretical tool to study different properties of simpler[17,19] and complex[19] clusters of this family, niobium,[15]

* To whom correspondence should be addressed. Tel +34 964728083 Fax: +34 964728066 e-mail: andres@exp.uji.es

10.1021/jp011535x CCC: $20.00
Published on Web 10/03/2001

chromium,[24] manganese,[25,26] iron [27] oxide clusters, and other metal compounds.[28−30]

The topological analysis of the ELF of Becke and Edgecombe[31] provides a convenient partition of the molecular space into basins of attractors which can be interpreted on the basis of the simple Lewis's model of chemical bonding.[32] This methodology has been proved to be a powerful tool for the description of chemical bonding in a great variety of chemical systems.[16,33−36] It is based on the excess local kinetic energy due to Pauli repulsion, and therefore is able to recognize which regions of a molecule present an antiparallel spin pair behavior, as introduced by Savin et al..[37]

The ELF gradient field defines localization attractors, each one surrounded by a three-dimensional space called a basin. Basins are characterized by their synaptic order, which corresponds to the number of cores to which they are connected. Thus, zero-order basins, $C(X_i)$ (X_i represents the atomic label), are called core basins and contain a nucleus; monosynaptic basins $V(X_i)$ are associated to lone pairs; disynaptic basins $V(X_i,Y_i)$ are connected to two core basins $C(X_i)$ and $C(Y_i)$, and correspond to a covalent bond, and so on. The resulting isosurfaces of the ELF density are consistent with the Lewis and VSEPR pictures of bonding,[38] they have been used to characterize lone pairs in a variety of situations recently by Chesnut[34] and applied extensively by Silvi and Savin and their collaborators.[16,18,32,39−41]

Upon the increase of the value of ELF, η, defining the bonding isosurface, a reducible domain splits into several domains each containing less attractors than the parent domain. The reduction of localization occurs at a turning point, which is a critical point of index 1 located on the separatrix of two basins involved in the parent domain. Ordering these turning points (localization nodes) by increasing η enables us to build tree-diagrams reflecting the hierarchy of the basins. A detailed description of the mathematical and quantum formulation of this method has been previously described.[38]

The integration of the density over the basins has been performed with the TopMod program.[42] The algorithms used for these calculations were recently published.[43] The calculation of basins populations provides an indication of the electron density involved in a particular bond. Besides, fluctuation (or variance) is related to the electron delocalization of a basin; the expression of the variance in terms of the contributions arising from the other basins is called covariance. Therefore, the topological partition of the electron density yields an alternative method for a chemical bonding analysis.[18]

3. Results and Discussion

Structures of the different minima on potential energy surfaces for $V_xO_y^+$ and V_xO_y ($x = 2-4$, $y=2-10$) clusters and the atoms numbering are displayed in Figures 1 to 9. The low-lying spin states, i.e., singlet and triplet, or doublet and quadruplet, of a given model were considered in the calculations. Detailed discussion on the structural properties, relative stability, dissociation energies, vibrational frequency analysis, and nature of the bonding based on Mulliken charges and ELF topological analysis of the different clusters are given in the following subsections.

3.1. Optimized Geometries and Relative Energies. a) $V_2O_2^+$ and V_2O_2. Three different structures have been calculated for both cationic and neutral systems: a bent OVOV (model A), appearing only for $V_2O_2^+$ systems; a four-membered ring V_2O_2 (model B); and an arrangement of a O_2 and a V_2 unit O_2-V_2 (model C). The structure B is the most stable in both cases. This structure in the cationic system presents C_s symmetry and its ground-state is $^2A'$. The OVOV bent structure possesses C_s symmetry, and a quadruplet electronic state $^4A'$ has been characterized. The O_2-V_2 adduct is found to be very unstable: quadruplet ^4A has a relative energy of 177.84 kcal mol^{-1}, very close to the excited $^2A'$ electronic state.

The most energetically favorable system for neutral clusters is the four-membered ring with C_{2v} symmetry in its $^3A_1$ electronic state. Two singlet-excited electronic states, ^1A_g and $^1B_{1u}$, have been located at 7.29 and 63.45 kcal mol^{-1} respectively, possessing D_{2h} symmetry. $O_2^-V_2$ structures present C_s symmetry both the triplet $^3A'$ state and the less stable singlet $^1A''$. For model C, on going from triplet, $^3A'$ to singlet $^1A''$, a change in the geometry is found and it becomes a planar structure, in particular a decrease of the V1−O1 bond length and an increase of the V2−O2 bond length is found. The addition of an electron to the most stable cation, model B, produces a rearrangement of the V−O bond lengths to generate a OVO fragment interacting with a vanadium atom, according to the respective V−O distances; while for the model C, an increase of the O−O bond length as well as a decrease in the V−O distance is observed and a planar arrangement is obtained.

b) $V_2O_3^+$ and V_2O_3. An open OVOVO structure (model A) and a four-membered ring OV_2O_2 arrangement (model B) were studied, the latter being the most stable for both cation and neutral clusters. For $V_2O_3^+$, model B ground-state presents C_s symmetry and $^2A'$ electronic state, with a quasi-planar four-membered ring. An excited electronic state $^4A''$, very close in energy, has been also characterized. Two bent models have been calculated, with symmetry C_{2v} ($^4A_2$), and C_1 (^2A). No significant differences in geometry are found between the ground and the excited electronic state in model B.

Neutral OV_2O_2 species show C_s symmetry with a nonplanar ring for the $^3A'$ state and a quasi planar ring the singlet $^1A'$. The excited $^1A'$ is 25.74 kcal mol^{-1} higher in energy than the ground-state. An OVOVO structure has been located with C_2 symmetry and ^3B electronic state. It shows a short V−V distance of 2.465 Å, indicating a metal−metal interaction. No minimum was found for a singlet electronic state.

The addition of an electron to the cations clearly affects geometry, changing from a planar to a puckered ring in model B, as well as enhancing the vanadium- vanadium interactions in the A open structures.

c) $V_2O_4^+$ and V_2O_4. The most stable conformation of V_2O_4 clusters has been found to be a four-membered ring, OVO_2VO (model B). An open $OVOVO_2$ structure, model A, and a four-membered ring VO_2VO_2 (model C) have also been characterized. Model B ground-state ($^2A'$) in the cationic form has C_s symmetry, and an excited $^4A''$ electronic state has also been characterized. It does not present significantly different V−O bond lengths, although it presents a nonplanar ring conformation. Model A doublet electronic state is 29.69 kcal mol^{-1} more energetic than model B. The VO_2VO_2 structure in its ground-state $^2B_2$ belongs to the C_{2v} spatial group and has a relative energy of 40.32 kcal mol^{-1}.

Neutral species have C_{2v} symmetry for model B. The ground-state presents a quasi-planar ring while the excited-state becomes a puckered ring. The geometrical parameters of the $^3B_2$ ground-state are similar to the reported values of Vyboishchikov and Sauer.[19] A linear arrangement corresponding to the model A, (^3A) $OVOVO_2$, has been characterized with a relative energy of 29.10 kcal mol^{-1}. Model C presents C_{2v} symmetry for both ground $^3B_1$ and excited $^1A_1$ electronic states. In both B and C models, the triplet electronic state is more stable than the singlet

state. Important geometrical rearrangements are not observed on going from ground to exited electronic states, therefore a change in the vanadium atoms electronic configuration is expected. This change depends on different types of interaction, i.e., electron repulsion, ferromagnetic-antiferromagnetic transformation, etc. Vyboishchikov and Sauer[19] point out the importance of this magnetic coupling to understand the behavior of these systems by using the "broken-symmetry" approach. This analysis is not evident in the DFT scheme and goes beyond the scope of this paper.

The addition of an electron to the cationic systems originates the variation in vanadium-bridging oxygen bond lengths, as well as a nonplanar conformation for the four-membered ring in models B.

d) $V_2O_5^+$ and V_2O_5. An open O_2VOVO_2 model (model A) and a four-membered ring, OVO_2VO_2 (model B), have been localized as minima in the potential energy surface, the latter being the most stable one. The ground-state $^2A''$ corresponds to a planar ring with two different terminal oxygen−vanadium distances, about 1.56 and 1.70 Å. A puckered ring-based structure is a low-lying electronic state ($^4A'$). Thus, a conformational change is observed for this electronic transition. Open model A presents two minima for electronic states ^2A and ^4A. A third structure, model C, consisting of three bridging oxygens and C_{3v} symmetry has been characterized as a saddle point of index two, the imaginary frequencies of −133 and −127 cm^{-1} are associated to the transfer of a bridging oxygen between the two vanadium centers, becoming model B.

For neutral clusters the same trend in relative energies is found. Model B consists of a quasi-planar ring for both electronic states with a V−O bond distance for terminal oxygens and two for ring oxygens. The geometrical parameters of the ^1A ground-state are similar to the reported values of Vyboishchikov and Sauer.[19] The O_2VOVO_2 structure presents V−O terminal bond lengths around 1.60 Å, whereas bridging oxygen is bonded differently to the two vanadium centers. Model C has also been computed and a saddle point of index two, similar to the cationic one is obtained, with relative energy of 6.89 kcal mol^{-1}. When an electron is added to the cations, no significant differences in geometry are observed.

e) $V_2O_6^+$ and V_2O_6. Two cyclic models (A and B) and a linear model (model C) were calculated. Model A involves a quasi-planar four-membered ring with two terminal oxygens on each vanadium center. Three long and one short vanadium-terminal oxygen distances are present. This structure has a C_s symmetry and corresponds to a doublet $^2A''$ electronic state. A quadruplet C_1 puckered ring-based structure has been found on the potential-energy surface, with similar distances and very close in energy to the former. Model B is also a four-membered ring with two terminal oxygens and an O_2 unit. The most stable conformation for $V_2O_6^+$ is a doublet electronic state (^2A), very close in energy to a ^4A state. Both states present similar geometrical parameters, but a difference in the O_2 unit-vanadium atom (V1) distance is found (1.879 Å versus 2.199 Å). The O−O distance is 1.242 Å for the doublet electronic state and 1.214 Å for the quadruplet electronic state. These findings lead us to consider two different O_2-vanadium interactions. Calculated O_2 and O_2^- distances are 1.215 and 1.353 Å, respectively. From now on, we will refer to these systems as molecular oxygen for O_2 and superoxo for O_2^-. An open geometry has been considered, involving a bridging oxygen, three terminal oxygens and a O−O unit. The ^2A and the ^4A electronic states are very close in energy, and the changes in O−O and O5−V1 bond lengths observed for model B are also observed for these clusters.

V_2O_6 structures show larger stability for open-shell systems. The model A triplet state is the most stable one. Again, two different terminal oxygens are found; this arrangement is very similar to the values recently obtained by Vyboishchikov and Sauer.[19] The singlet state is a D_{2h} arrangement with four terminal oxygen−vanadium bond lengths of 1.638 Å. Model B in its ^3A electronic state presents an O−O distance of 1.317 Å, and a singlet electronic state presents similar geometrical parameters. A superoxo-vanadium interaction is proposed for both systems. The open model C presents similar geometries for both singlet and triplet states, and a superoxo interaction is assigned. The addition of an electron to the cationic systems involves basically the change of terminal oxygens-vanadium distances, as well as the decrease of the O_2−V1 distances (an enhancement of the interaction between the O_2 fragment and the vanadium atom).

f) $V_2O_7^+$ and V_2O_7. The addition of an oxygen atom to V_2O_6 models leads to two different arrangements for clusters with stoichiometry V_2O_7. Model A $V_2O_7^+$ involves a planar four-membered ring and three terminal oxygens, as well as an O_2 unit, corresponding to $^2A''$ and $^4A''$ degenerate electronic states with identical geometrical parameters; however, an increase of a terminal oxygen−vanadium distance is observed. The bond length associated to the interaction with the O_2 unit is 2.143 Å, and the O−O bond length is 1.213 Å, very close to the calculated O_2 value of 1.215 Å. A linear structure involving two O_2 units has also been considered, Model B. It is more energetic than the most stable ring structure at the ^2A electronic state. Two different arrangements for the O_2 units are observed: first, a O−O distance of 1.236 Å and a O_2−V1 distance of 1.887 Å, and the second involving O−O distance of 1.316 Å and V2−O distance of 1.938 Å. The former corresponds to a superoxo-vanadium interaction while the latter is assigned to a peroxo-vanadium interaction, being the calculated peroxo O_2^{2-} bond length, 1.618 Å.

For neutral systems, model A presents a triplet $^3A''$ ground-state with C_s symmetry and a vanadium V1 interacting with both oxygen atoms of the O_2 unit, corresponding to a peroxo-vanadium interaction. A comparison with the calculated structure of Vyboishchikov and Sauer[19] renders similar values of the geometrical parameters, although these authors give a fundamental singlet electronic state. Bond lengths are quite similar to those obtained for cationic systems. A closed-shell state has been also characterized, binding the O_2 unit to a terminal oxygen. This structure presents two terminal oxygens, two ring oxygens belonging to a four-membered ring, and a O_3 unit. An open structure, called model B, involves two different O_2 units: V1 interacts with a superoxo unit while V2 interacts with a peroxo unit. Almost identical geometries are found for the triplet and the singlet electronic states. The addition of an electron to the cations makes the peroxo interaction dominant, instead of the molecular interaction.

g) $V_3O_6^+$ and V_3O_6. Three different models were considered: a six-membered ring (model A), a linear-open structure (model B), and a four-membered ring (model C), see Figure 7. The most stable one is model A, involving a six-membered ring with terminal oxygens attached to the vanadium centers, symmetry C_s, and electronic state $^3A''$. It adopts a ship conformation with terminal oxygen−vanadium distances of about 1.55 Å, and ring oxygens-vanadium distances in the range of 1.7−1.9 Å. A singlet C_{3v} structure with electronic state $^1A_1$ has been characterized, very close in energy. The following

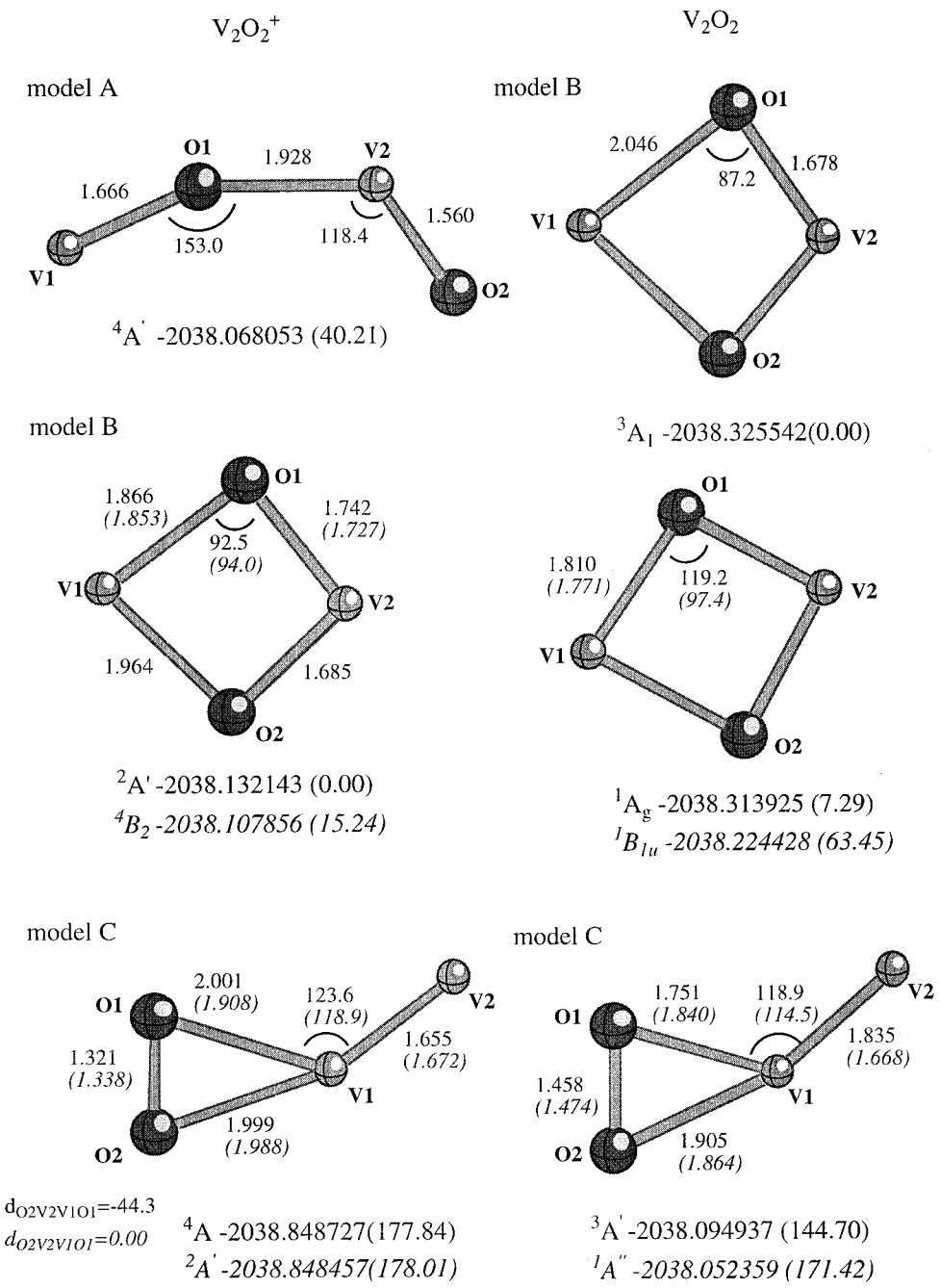

Figure 1. Geometrical parameters (bond lengths in Å and angles in degrees) and relative energies in kcal mol^{-1} for $V_2O_2^+$ (left) and V_2O_2 (right) clusters. Values in parentheses correspond to the least stable system.

model in energy is model C, consisting of a quasi-planar four-membered ring with an O and a VO_3 unit bonded to the vanadium atoms. A triplet electronic state is again the most stable one, with a quasi-planar ring. However, ^{1}A excited electronic state presents a nonplanar ring. Finally, the most stable linear structure corresponds to a ^{3}A electronic state. No significant changes in geometry are found between these electronic states. Thus, cationic $V_3O_6^+$ family prefers open-shell configurations and no important differences in geometry are present between ground and excited electronic states, except for the change in the dihedral angle of model C.

For neutral systems the same models were considered, model A being the most stable one in its ^{4}A′ electronic state. It possesses C_s symmetry, quasi-planar ring conformation, and two different ranges of V−O bond lengths appear corresponding to terminal and ring oxygen−vanadium bonds. In a narrow window of energy the doublet ^{2}A′ electronic state is characterized, having C_s symmetry and no important differences in bond distances regarding the quadruplet. However, the ring adopts now a chair conformation and O1 and O4 stay in a plane above the vanadium atoms, while oxygens O3 stay below. Model C presents a quasi-planar four-membered ring and very similar V−O distances for both quasi-degenerate ^{2}A and ^{4}A electronic states. Linear model B presents two electronic states, ^{4}A and ^{2}A′.

h) $V_3O_7^+$ and V_3O_7. Based on the $V_3O_6^+/V_3O_6$ structures, four different models for this stoichiometry have been considered. The addition of an oxygen atom to the six-membered ring structure leads to model A, where identical conformation is obtained and the extra atom is placed in the same plane as the terminal oxygens, centered in the ring (C_{3v} symmetry). The ground-state in the cationic form is a singlet, ^{1}E. Excited C_s structure, corresponding to a ^{3}A″ electronic state, higher in

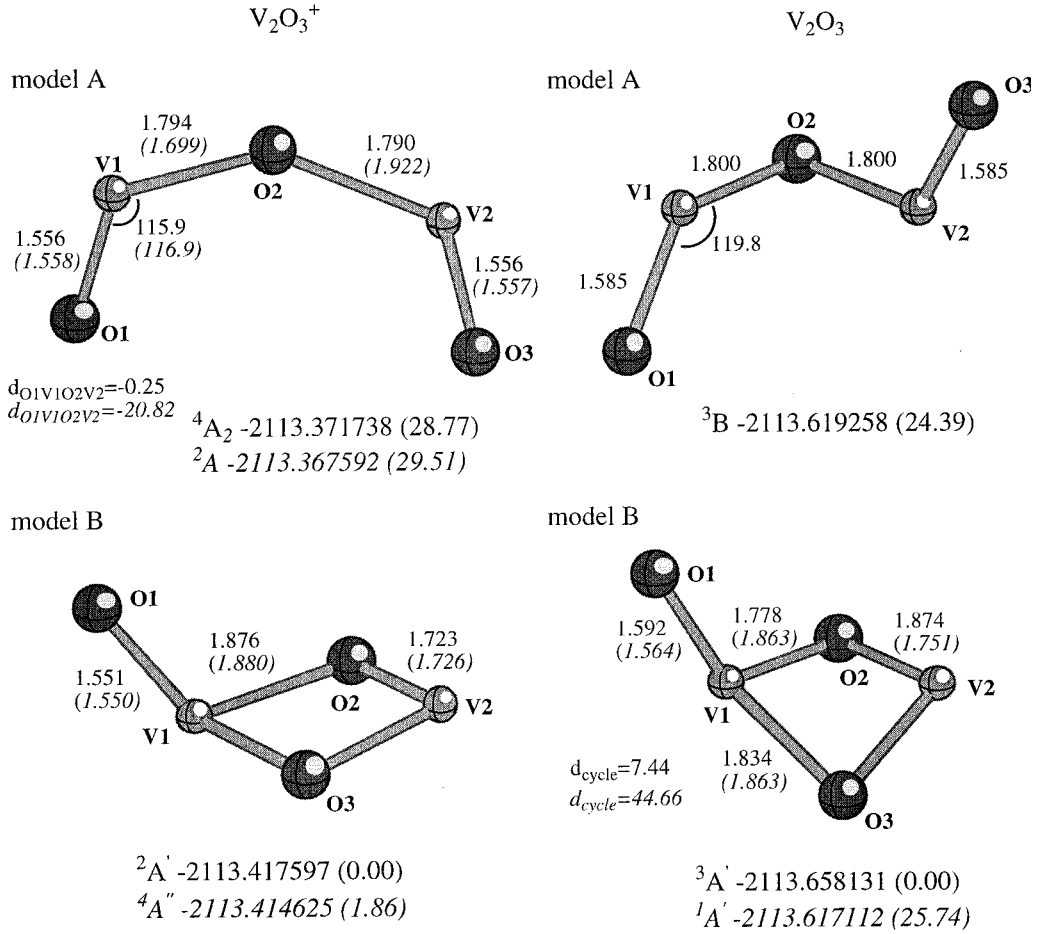

Figure 2. Geometrical parameters (bond lengths in Å and angles in degrees) and relative energies in kcal mol^{-1} for $V_2O_3^+$ (left) and V_2O_3 (right) clusters. Values in parentheses correspond to the least stable system.

energy. Two different terminal oxygens-vanadium distances are found, as well as for bridging oxygens-vanadium bonds. The distance O5−V1 slightly increases on going from singlet to triplet electronic state; however, an opposite trend is found for the O5−V2 distance. The low-lying excited state corresponds to model C2, showing a four-membered V_2O_2 ring with one terminal oxygen bonded to each vanadium atom, together with a VO_3 unit. Model C1 involves two terminal oxygens on the same vanadium atom V1. A long distance is present between the ring oxygens O3 and O4 and this V1 center. Model B presents a branched structure and two different terminal oxygens are found. The V1−O2−V2 angle is approximately 180 degrees. This model is the least stable of all the considered models. No open shell has been calculated for models B, C1, and C2.

Regarding neutral systems, Model A is again the most stable structure, with a $^2A''$ ground-state of C_s symmetry. The quadruplet state has been calculated to be 52.31 kcal mol^{-1} more energetic than the ground-state, and being significantly distorted. The arrangements found for models C1 and C2 of both cationic and neutral systems are similar, the oxygen atom attached to V2, model C2, is more stable than the oxygen linked to V1, model C1. Only singlet electronic states were considered. Linear model B presents a C_s symmetry with four terminal oxygens and three bridging oxygens. This model is very unstable in comparison with the six-membered ring. No significant differences in geometry are observed when comparing cations and neutral systems, except for the loss of the symmetry in model A and the bridging oxygen−vanadium V1−O2 and V2−O2 bond lengths in model B.

i)V_4O_{10}. In Figure 9 the neutral system corresponding to a tetrahedral cage is depicted. No cationic minima were found for this stoichiometry. This structure presents ^1T_d symmetry. Four equivalent terminal oxygens are found, as well as six equivalent bridging oxygens. Only singlet electronic state was converged, corresponding to the $^1T_2$ electronic state. These values are very similar to the theoretical results of Vyboishchikov and Sauer.[19]

In summary, different V−O distances are found in these compounds. A short bond length of 1.550 Å is present for terminal oxygens, and it is associated to a double bond or a vanadyl bond.[44] A medium V−O distance of 1.70−1.80 Å is present for bridging oxygens, and corresponds to a single bond. A long-range interaction is present when a distance of 1.9−2.2 Å is found, as for V−O_2 interactions. Bulk V_2O_5 material present the following V−O distances:[45] 1.58 Å for the vanadyl bond, 1.77 and 1.88 and 2.02 Å for bridging oxygens. Structures containing a four-membered ring are stabilized, and planar conformations as well as puckered rings are found. Low multiplicities are preferred for cations, except for the $V_3O_6^+$ systems which prefer a triplet electronic state. Neutral systems prefer high multiplicities except for V_2O_5 and V_3O_7 systems, where a closed-shell and a doublet electronic state are the most stable conformations, respectively.

3.2. Dissociation Channels, Ionization Potential, and Binding Energies. The dissociation or fragmentation energy has been evaluated as the difference of the total energy of the cluster and the energy sum of the fragments resulted from the corresponding dissociation channels. The results obtained for

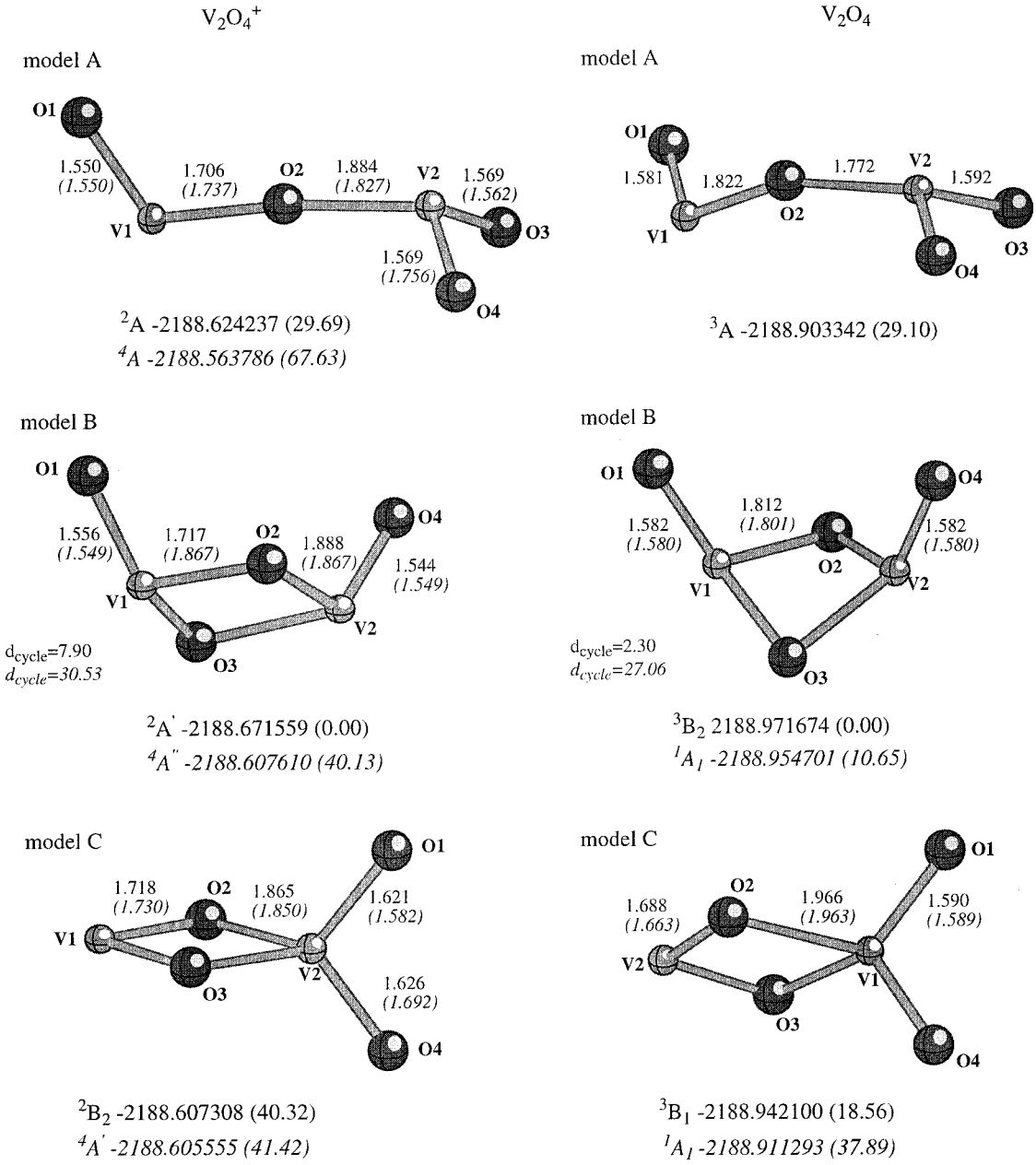

Figure 3. Geometrical parameters (bond lengths in Å and angles in degrees) and relative energies in kcal mol^{-1} for $V_2O_4^+$ (left) and V_2O_4 (right) clusters. Values in parentheses correspond to the least stable system.

the most stable clusters are presented in Table 1; Supporting Information 1S includes the dissociation channels for all the models studied. An analysis of these data shows that the stability order is dependent on model systems and fragmentation products. The most exothermic processes are associated to the generation of VO, VO^+, VO_2, VO_3 and O_2, constituting the building blocks for larger moieties. V_2O_4 and V_2O_5 in their four-membered ring arrangement are found to be the building blocks for bigger clusters such as V_2O_6 and V_2O_7. Linear structures such as V_2O_4, V_2O_5 model A and V_3O_6, V_3O_7 model B are unstable species and would tend to decompose into smaller fragments, as their small endothermic and even exothermic values of dissociation energies show. On the contrary, compact models involving alternating V−O bonds are expected to be more stable, as in V_2O_5 model B or V_3O_6 model A. This last case illustrates the order in stability: six-membered ring > four-membered ring > linear structure. Among four-membered ring structures, the case of $V_3O_7^+$ shows that a tetrahedral environment is favorable when only one terminal oxygen is present. This arrangement is found in the bulk material.

Ionization potential (IP), calculated as the difference between the ionic and the neutral total electronic energies, increases when increasing the content in oxygen. Thus, the result for V_2O_x is V_2O_2 (5.26) < V_2O_3 (6.55) < V_2O_4 (8.17) < V_2O_5 (9.78), in eV. If another oxygen is added, the result is a decrease in the IP value, for V_2O_6 9.56 eV while the IP value of V_2O_7 is 10.06 eV. For V_3O_y clusters, the same trend is observed and a slight increase in the IP value is obtained, 8.26 and 8.96 eV for V_3O_6 and V_3O_7 clusters, respectively. Therefore, neutral compounds having a larger content in oxygen show larger values of IP.

The decomposition energy of V_xO_y clusters into smaller V_xO_{y-1} clusters and O atom (DEO) has been calculated as the total energy of the V_xO_{y-1} cluster plus the energy of an isolated oxygen atom minus the energy of the V_xO_y cluster. The calculated values of DEO for the most stable clusters are reported in Table 2. An analysis of the results renders that the

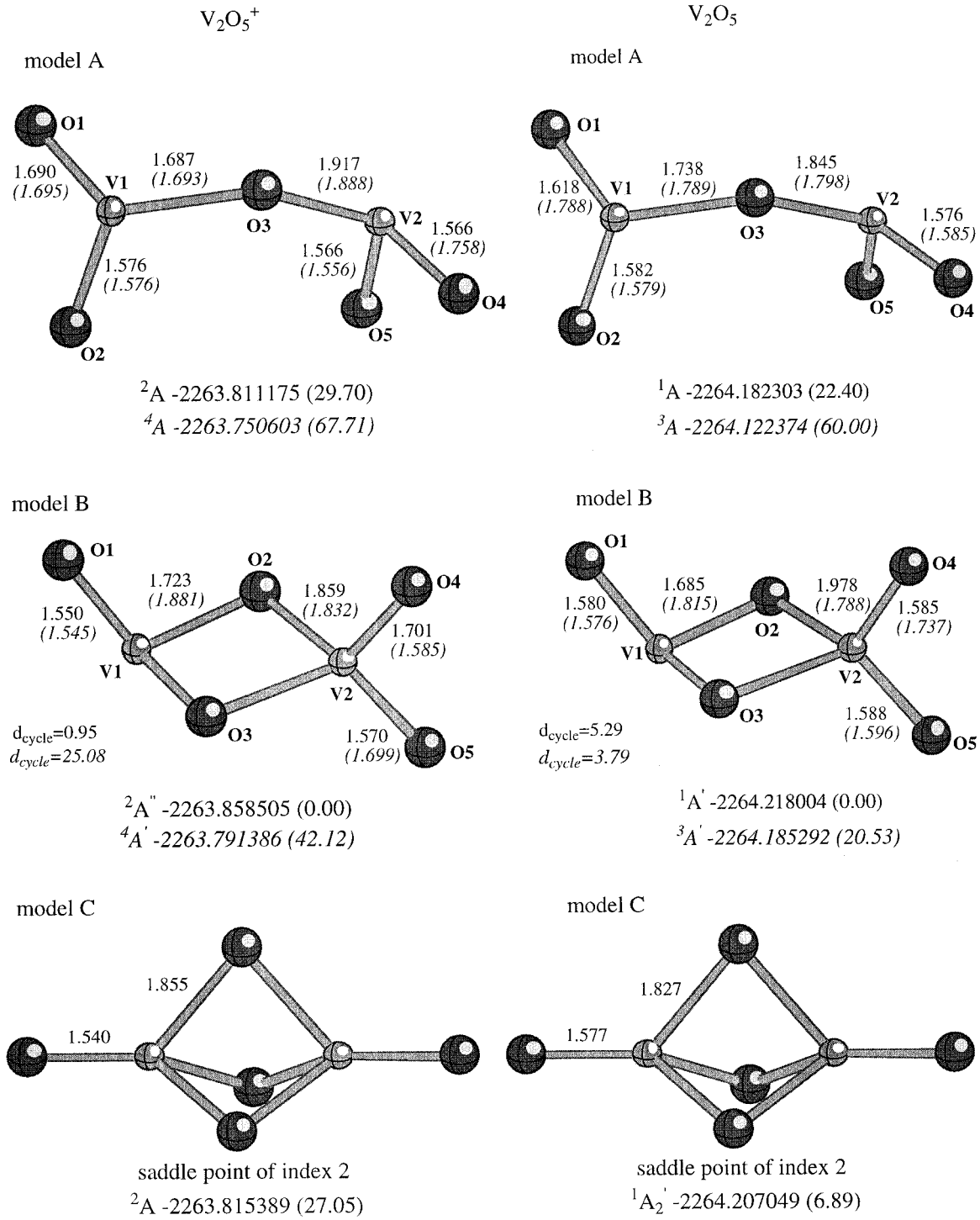

Figure 4. Geometrical parameters (bond lengths in Å and angles in degrees) and relative energies in kcal mol^{-1} for $V_2O_5^+$ (left) and V_2O_5 (right) clusters. Values in parentheses correspond to the least stable system.

addition of an oxygen atom to small clusters to form clusters richer in oxygen is thermodynamically favorable. Thus, clusters with a high content in oxygen like V_2O_6 and V_2O_7 show small values of DEO, indicating that decomposition into V_2O_5 and V_2O_6 clusters plus atomic oxygen is little endothermic and therefore less difficult. Analogous analysis can be done for the study of the capability of losing an O_2 molecule. Decomposition energy losing O_2 (DEO_2) is analogously calculated and is shown in Table 2. Again, V_2O_6 and V_2O_7 clusters present a higher tendency to lose O_2 and become V_2O_4 and V_2O_5 clusters, as it was suggested from the geometrical analysis and the fragmentation channels. We conclude that V_2O_4 and V_2O_5 systems are the most stable clusters.

Finally, regarding the fragmentation channels, VO_2, VO_3, VO, VO^+, and O_2 are the most stable fragments of $V_2O_y^+$ and V_2O_y systems, and V_2O_4 and V_2O_5 stoichiometries are the building blocks of the larger clusters. Nevertheless, dissociation channels depend on the products and model. Ionization potentials increase with a high content in oxygen, and decomposition energies render that V_2O_6 and V_2O_7 compounds tend to lose O and O_2 and become stable V_2O_4 and V_2O_5 systems. These results are in agreement with experimental results reported by Bell et al.,[8]

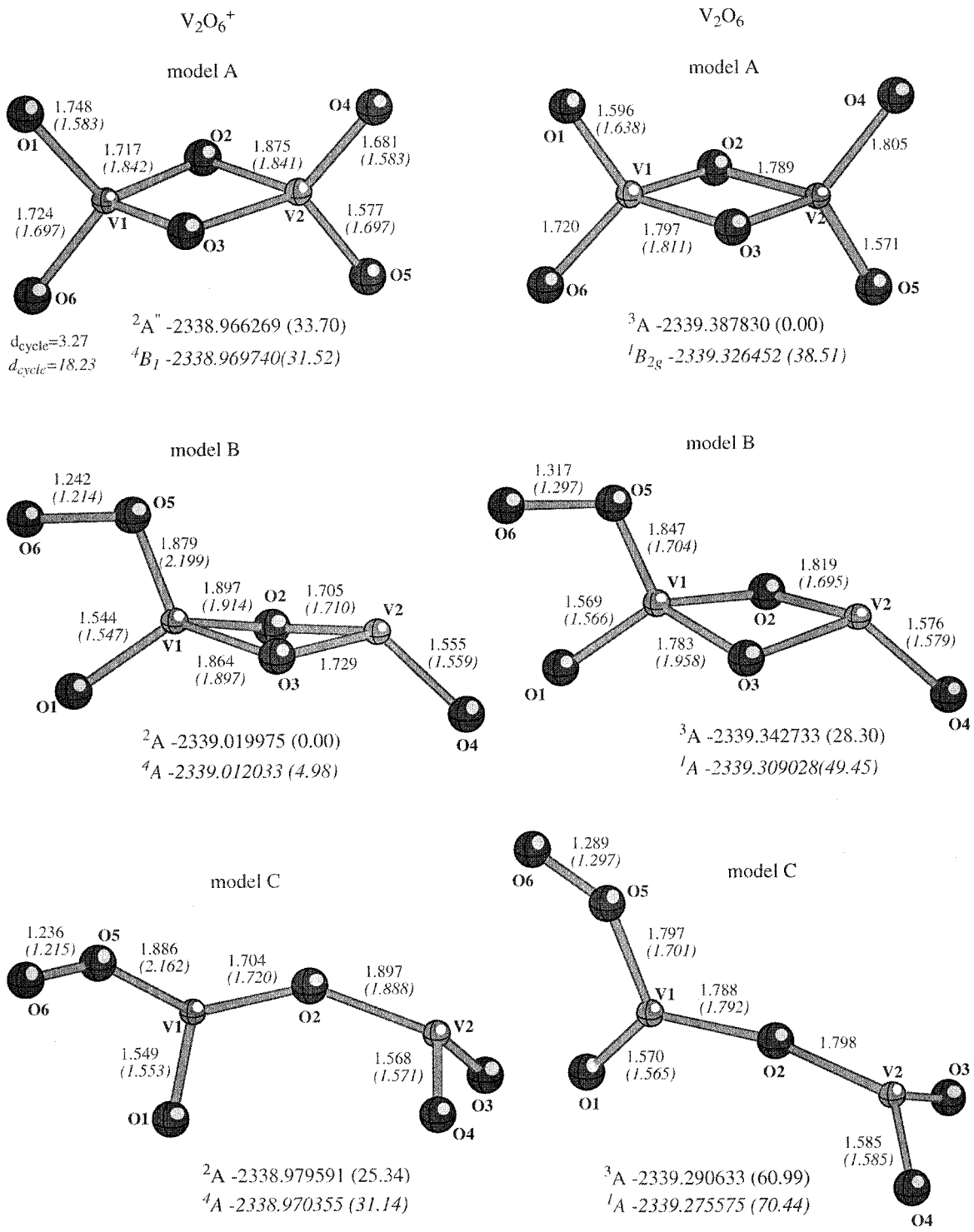

Figure 5. Geometrical parameters (bond lengths in Å and angles in degrees) and relative energies in kcal mol^{-1} for $V_2O_6^+$ (left) and V_2O_6 (right) clusters. Values in parentheses correspond to the least stable system. A saddle point of index 2 has been found for model C in both cationic and neutral clusters.

where these authors identify VO_2, VO_3, V_2O_4, and V_2O_5 as the building blocks for larger systems. Clusters with high content in oxygen like V_2O_6 and V_2O_7 easily lose O_2.

3.3. Vibrational Frequency Analysis. The frequencies calculated at the harmonic level and the corresponding intensities for V_2O_y and $V_{3-4}O_y$ are listed in Supporting Information 2S and 3S. The calculated values of these frequencies are not scaled. Recently, Bytheway and Wong[46] have proposed a scale factor of 0.9929 for the B3LYP//6-31G* calculation level. An analysis of the vibrations with the highest intensities has been carried out. For all models, low frequencies are associated with bending modes and dihedral angles vibrations.

Open structures present an intense band associated to the vibration of the bridging oxygen between two vanadium atoms, at approximately 950 cm^{-1}. This is the case of V_2O_4, V_2O_5 model A, and V_3O_6 and V_3O_7 models C. Four-membered ring-based compounds present bands in the range of 400−700 cm^{-1} associated with ring oxygens-vanadium stretching and bending modes, as in V_2O_4, V_2O_5 models B, and V_3O_6 and V_3O_7 models C2. An exception is cationic and neutral V_3O_7 model C1, where

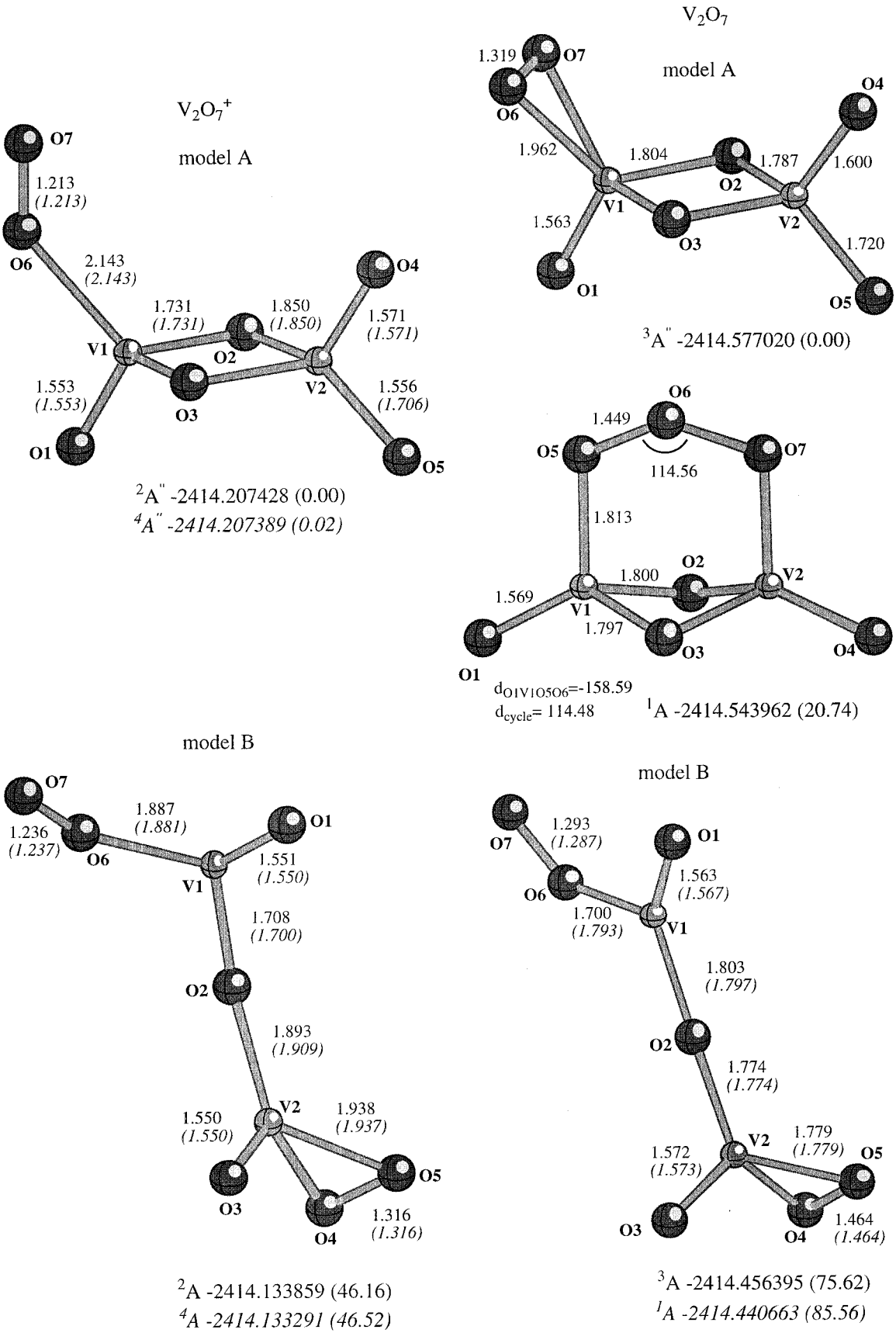

Figure 6. Geometrical parameters (bond lengths in Å and angles in degrees) and relative energies in kcal mol^{-1} for $V_2O_7^+$ (left) and V_2O_7 (right) clusters. Values in parentheses correspond to the least stable system.

no 600−700 cm^{-1} bands are found, and can be considered an arrangement of smaller VO_2 and VO_3 clusters, in agreement with the geometrical parameters. Terminal oxygens present characteristic frequencies at values higher than 1100 cm^{-1}. Among them, vanadium centers connected to two terminal oxygens present lower frequencies (about 1100 cm^{-1}) than those

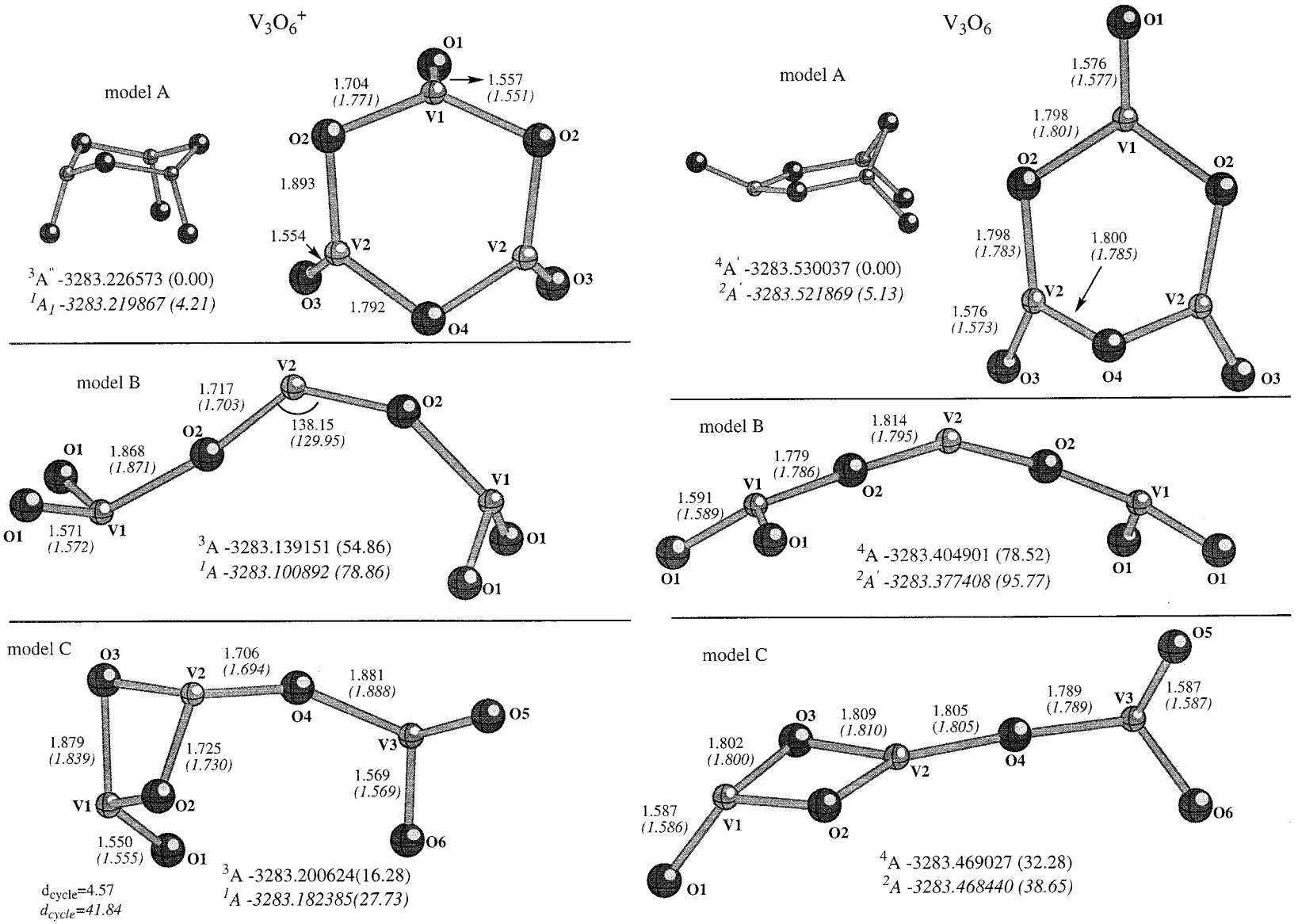

Figure 7. Geometrical parameters (bond lengths in Å and angles in degrees) and relative energies in kcal mol^{-1} for $V_3O_6^+$ (left) and V_3O_6 (right) clusters. Values in parentheses correspond to the least stable system.

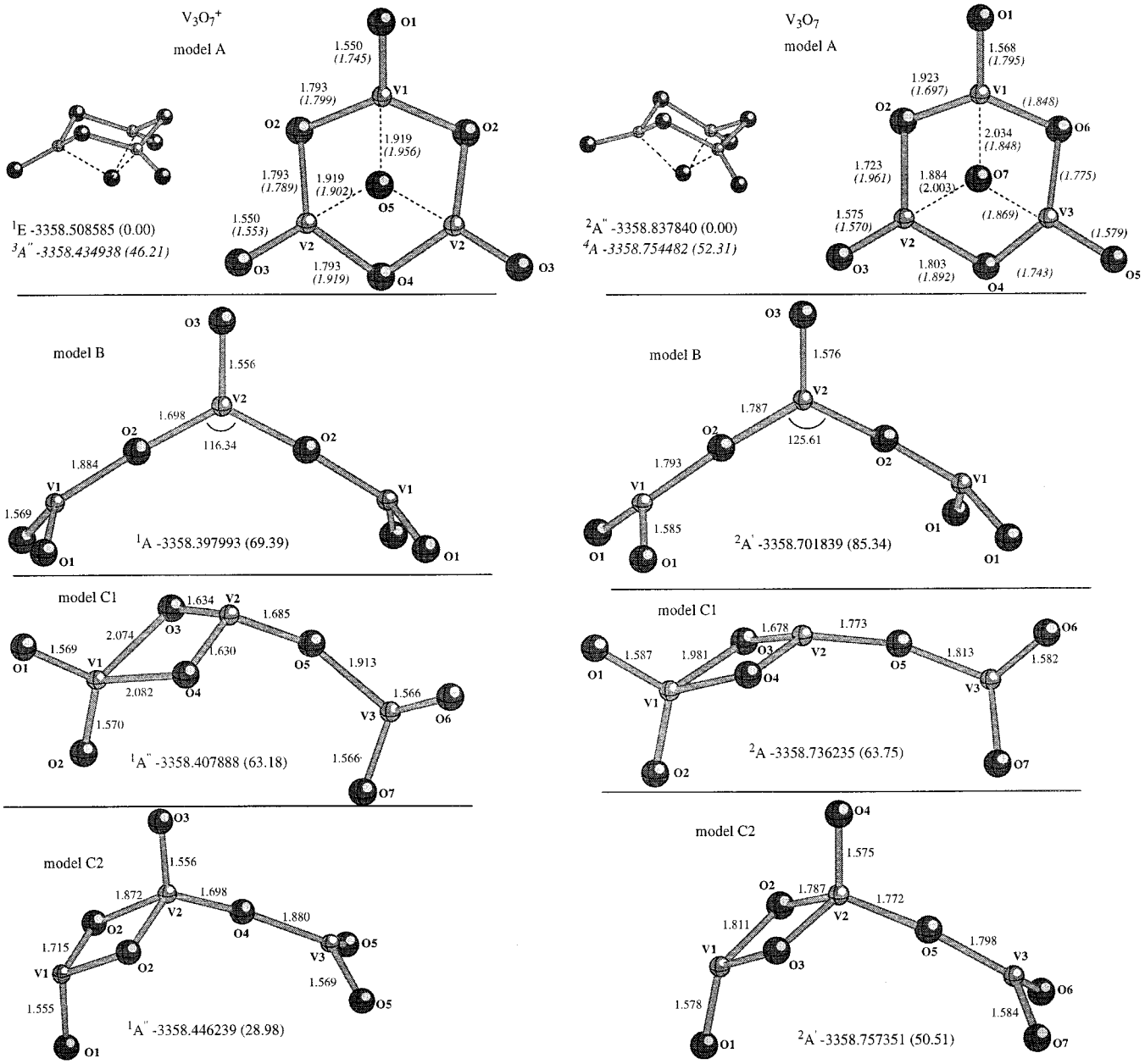

Figure 8. Geometrical parameters (bond lengths in Å and angles in degrees) and relative energies in kcal mol^{-1} for $V_3O_7^+$ (left) and V_3O_7 (right) clusters. Values in parentheses correspond to the least stable system.

bonded to only one (1150 cm^{-1}): V_2O_5 model B and V_3O_7 C2 illustrate this fact. Clusters containing O_2 units present a O−O stretching vibration at values of 1300−1600 cm^{-1}. In particular, superoxo O_2^- units vibrate at 1300 cm^{-1}, peroxo O_2^{2-} units at 675 cm^{-1}, and molecular O_2 units at 1600 cm^{-1}, approximately. As a reference, the calculated isolated O_2 molecule presents a bond length of 1.215 Å and a frequency of 1658 cm^{-1}; superoxo O_2^- possess a bond length of 1.353 Å and the frequency is 1211 cm^{-1}, and peroxo O_2^{2-} bond length is 1.618 Å and the frequency is 675 cm^{-1}.

3.4. Mulliken Population, Oxidation States and Topological Analysis. Some interesting observations emerge from the Mulliken populations analysis. Table 3 presents the atomic Mulliken charge and the atomic spin density for the most stable $V_xO_y^+/V_xO_y$ clusters.

Cationic systems present higher values for vanadium charges and lower values for oxygen charges than the corresponding neutral compounds. Vanadium atoms always possess positive Mulliken charges in the range of 1.10−1.50 electrons, although in some cases lower charges are found, i.e., V_2O_2 models B and C. Oxygen atoms present Mulliken charges in the range of −0.40 to −0.70 electrons except for systems possessing peroxo and superoxo fragments, as in $V_2O_6^+$ model B, where positive values for oxygen charges are found. These systems present O−O bonds so as to avoid an oxidation state higher than (+5) for vanadium. Among oxygen atoms, one can find that terminal oxygen atoms possess a lower negative charge than bridging or ring oxygen atoms. There is a close relationship between the values of the V−O distance and the negative charge on O atom: the shorter the V−O distance is, the more negative the charge on oxygen atom. Thus, Mulliken charges in the range of −0.30 and −0.35 electrons correspond to double and single terminal V−O bonds, respectively; bridging oxygens present charges of about −0.60 electrons. The central atom in V_3O_7 system's model A exhibits a very negative Mulliken charge due to the interaction with three vanadium atoms.

Three different O_2−V interactions can be found, in agreement with geometrical and vibrational results. The superoxo unit

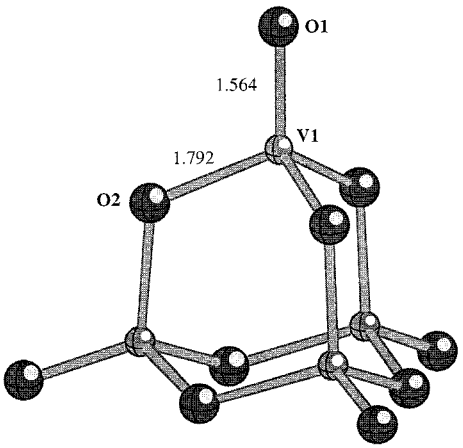

Figure 9. Geometrical parameters (bond lengths in Å and angles in degrees) and relative energies in kcal mol^{-1} for V_4O_{10} cluster.

involves O−O distances of approximately 1.3 Å, as for V_2O_6 models B and C in doublet electronic states. A charge transfer of 0.4 electrons from the vanadium-containing fragment to the O_2 unit is observed, and small negative Mulliken charges, or even positive values, are found for these atoms. The charge transfer is present for other systems containing a superoxo unit, like V_2O_7 model B oxygens O6 and O7. The peroxo unit in V_2O_7 compounds exhibits a charge transfer of 0.6 electrons from the rest of the molecule. Finally, a perturbed molecular O_2 fragment, present in $V_2O_6^+$ models B and C in ^4A electronic state, as well as in $V_2O_7^+$ model A, is characterized by a rather small charge transfer of 0.1 electrons from the O_2 unit to the vanadium-containing unit. V_2O_7 model A singlet electronic state shows a charge transfer of 0.72 electrons to the O_3 unit.

Regarding the spin density, different trends are observed. In general, vanadium atoms have the highest values of spin density, i.e., unpaired electrons are located in vanadium 3d orbitals. This is the case for small systems such as V_2O_2 and V_2O_3; they present similar geometries for low and high multiplicities, and spin density is located exclusively on vanadium centers, like in V_2O_2, V_2O_3, and V_3O_6. However, for a richer content in oxygen, spin density on oxygen centers is found. For example, V_2O_5 model B in its $^3A'$ shows the unpaired electrons on vanadium V1 and oxygen O4. On some occasions, like in $V_3O_7^+$ model A in its triplet electronic state, spin density is found on neighboring vanadium and oxygen atoms, corresponding to the break of a double V−O bond. When spin density is on oxygen atoms, it is located on terminal oxygens or on the superoxo unit as for $V_2O_6^+$ model B or V_2O_7 model B.

Oxidation states are also analyzed for all the clusters. If we consider an oxidation state of (−2) for oxygen atoms, small cationic and neutral clusters such as V_2O_2 and V_2O_3 would have formal oxidation states ranging from (+2) to (+3.5) (formally (+2), (+3) and (+4)) for vanadium atoms. $V_2O_4^+$ clusters are expected to show vanadium (+4 +5) oxidation states. In $V_2O_5^+$ clusters, however, a (+5 +6) oxidation state should appear, when the highest oxidation state for vanadium is (+5). Therefore, not all the oxygen atoms should be considered as (−2), but as (−1). These oxygens (−1) correspond to the largest values of terminal V−O bonds, while short V−O distances correspond to O (−2). When increasing the content in oxygen, O−O bonds appear in order to avoid vanadium oxidation states higher than (+5). Four-membered rings present vanadium oxidation states of (+4) and (+5), and correspond to the most stable structures, while linear or branched structures involve lower oxidation states and are unstable compounds. This is in agreement with the results of Bell et al..[8]

A topological bonding analysis based on the reduction of the localization domains as well as on the basins' population has been carried out for the most stable clusters. As shown in a

TABLE 1: Dissociation Channels and Its Corresponding Energies ΔE in EV for the Most Stable $V_xO_y^+$ and V_xO_y Cluster Models[a,b]

compound	dissociation channel	ΔE
$V_2O_2^+$ Model B ($^2A'$)	$VO_2 + V^+$	5.42
	$VO^+ + VO$	4.39
V_2O_2 Model B ($^3A_1$)	$VO_2 + V$	3.80
	2 VO	2.48
$V_2O_3^+$ Model B ($^2A'$)	$VO_2^+ + VO$	6.11
	$VO_2 + VO^+$	4.86
V_2O_3 Model B ($^3A'$)	$VO_3 + V$	6.75
	$VO_2 + VO$	4.24
$V_2O_4^+$ Model B ($^2A'$)	$VO_2^+ + VO_2$	5.73
	$VO^+ + VO_3$	5.68
V_2O_4 Model B ($^3B'_2$)	$VO_2 + VO_2$	5.48
	$VO^+ + VO_3$	6.22
$V_2O_5^+$ Model B ($^2A''$)	$VO_2^+ + VO_3$	4.72
	$VO_2 + VO_3^+$	6.59
V_2O_5 Model B ($^1A'$)	$VO_2 + VO_3$	6.08
$V_2O_6^+$ Model B (^2A)	$VO_3^+ + VO_3$	4.88
	$VO_2^+ + VO_2 + O_2$	6.50
V_2O_6 Model A (^3A)	2 VO_3	2.94
	2 $VO_2 + O_2$	6.42
$V_2O_7^+$ Model A ($^2A''$)	$V_2O_4^+ + O_2 + O$	4.22
	$VO_3^+ + VO_2 + O_2$	5.50
V_2O_7 Model A ($^3A''$)	$V_2O_4 + O_2 + O$	6.11
	$VO_2 + VO + O_2$	0.43
$V_3O_6^+$ Model A ($^3A''$)	$V_2O_5 + VO^+$	4.21
	$V_2O_4^+ + VO_2$	3.55
	$VO_3 + VO_2 + VO^+$	10.30
	$VO_2^+ + 2\ VO_2$	10.17
V_3O_6 Model A ($^4A'$)	$V_2O_5 + VO$	5.31
	$V_2O_4 + VO_2$	4.71
	$VO_3 + VO_2 + VO$	11.39
	$3VO_2$	10.19
$V_3O_7^+$ Model A (^1E)	$V_2O_5 + VO_2^+$	5.84
	$V_2O_4^+ + VO_3$	6.20
	$2VO_3 + VO^+$	11.87
V_3O_7 Model A ($^2A''$)	$V_2O_5 + VO_2$	6.38
	$V_2O_4 + VO_3$	6.99
	$VO_3 + 2VO$	12.47
V_4O_{10} ($^1T_2$)	$V_3O_7 + VO_3$	6.86
	$V_3O_6 + VO_2 + O_2$	12.62
	2 V_2O_5	7.16
	2 $V_2O_4 + O_2$	11.86

[a] The smallest fragments have the following ground electronic states: $VO^+(^3\Sigma)$, Vo_2^+ ($^1A_1$), $VO_3^+(^1A')$, $VO(^4\Sigma)$, $VO_2(^2A_1)$, $VO_3^+(^2A')$, $O(^3P)$, $O_2(^3\Sigma_g^-)$, $V^+(^5D)$, and $V(^4F)$. [b] Channels rendering V_xO_{y-1} + O and V_xO_{y-2} + O_2 fragments are shown in Table 2.

TABLE 2: Decomposition Energy in eV of the Most Stable Clusters Losing Atomic $O(^3P)$ (DEO) and Molecular $O_2(^3\Sigma_g^-)$ (DEO_2)

system	DEO	DEO_2
$V_3O_7^+$ (^1E)	6,02	
V_3O_7 ($^2A''$)	6,73	
$V_2O_7^+$ ($^2A''$)	3,45	0,79
V_2O_7 (^3A)	3,95	1,06
$V_2O_6^+$ (^2A)	2,74	0,77
V_2O_6 (^3A)	2,52	2,17
$V_2O_5^+$ ($^2A''$)	3,44	3,29
V_2O_5 ($^1A'$)	5,05	6,53
$V_2O_4^+$ ($^2A'$)	5,26	5,97
V_2O_4 ($^3A''$)	6,88	8,87
$V_2O_3^+$ ($^2A'$)	6,12	
V_2O_3 ($^3A'$)	7,40	

TABLE 3: Mulliken Net Atomic Charges (a.u.) and Spin Densities in Parentheses for the Most Stable $V_xO_y^+/V_xO_y$ Clusters

	Atom								
Model	V1	V2	O1	O2	O3	O4	O5	O6	O7
$V_2O_2^+$ (^{2}A)	1.16(3.0 0)	1.16(−2. 10)	−0.68(0. 08)	−0.64(0. 02)					
V_2O_2 ($^3A_1$)	0.58(3.8 5)	0.78(−2. 01)	−0.68(0. 08)	−0.68(0. 08)					
V_2O_3+ (^{2}A)	1.36(−1. 09)	1.25(2.0 9)	−0.34(0. 14)	−0.64(− 0.07)	−0.64(− 0.07)				
V_2O_3 (^{3}B)	0.87(1.1 0)	0.87(1.1 0)	−0.51(− 0.09)	−0.72(− 0.01)	−0.51(− 0.09)				
V_2O_3 (^{3}A)	1.14(−1. 08)	0.87(3.0 0)	−0.52(0. 09)	−0.75(0. 02)	−0.75(− 0.03)				
$V_2O_4^+$ (^{2}A)	1.45(0.0 0)	1.38(1.1 1)	−0.31(0. 01)	−0.61(0. 02)	−0.61(0. 02)	−0.31(− 0.15)			
V_2O_4 (^{3}A)	0.98(2.2 1)	1.30(0.0 3)	−0.50(− 0.19)	−0.77(− 0.05)	−0.50(0. 00)	−0.50(0. 00)			
V_2O_4 ($^3B_2$)	1.20(1.1 4)	1.20(1.1 4)	−0.48(− 0.10)	−0.72(− 0.03)	−0.72(− 0.03)	−0.48(− 0.10)			
$V_2O_5^+$ (^{2}A)	1.47(−0. 01)	1.42(−0. 31)	−0.28(0. 00)	−0.58(0. 01)	−0.58(0. 01)	−0.21(0. 93)	−0.25(0. 37)		
V_2O_5 (^{1}A)	1.35	1.28	−0.43	−0.63	−0.63	−0.46	−0.47		
$V_2O_6^+$ (^{2}A)	1.38(−0. 64)	1.45(−0. 03)	−0.29(0. 10)	−0.58(0. 00)	−0.60(0. 01)	−0.30(0. 00)	−0.17(0. 56)	0.11(1.0 1)	
V_2O_6 (^{3}A)	1.35	1.35	−0.36	−0.63	−0.63	−0.36	−0.36	−0.36	
$V_2O_7^+$ (^{2}A)	1.40(0.0 0)	1.42(0.3 0)	−0.29(0. 03)	−0.59(0. 00)	−0.59(0. 00)	−0.27(− 0.35)	−0.22(− 0.93)	−0.08(0. 79)	0.21(1.1 8)
V_2O_7 (^{3}A)	1.39(−0. 07)	1.35(−0. 28)	−0.38(0. 00)	−0.66(0. 01)	−0.66(0. 01)	−0.38(0. 38)	−0.34(0. 88)	−0.17(0. 53)	−0.17(0. 53)
$V_3O_6^+$ (^{3}A)	1.46(0.0 7)	1.35(1.1 3)		−0.33(0. 00)	−0.69(− 0.01)	−0.35(− 0.14)	−0.74(− 0.03)		
V_3O_6 (^{4}A)	1.21(1.1 5)	1.21(1.1 4)		−0.46(− 0.11)	−0.75(− 0.04)	−0.46(− 0.11)	−0.46(− 0.11)		
$V_3O_7^+$ (^{1}E)	1.43			−0.26	−0.60	−0.71			
V_3O_7 (^{2}A)	1.28(1.1 0)	1.36(0.0 2)		−0.42(− 0.14)	−0.67(0. 00)	−0.41(0. 00)	−0.67(0. 00)	−0.76(0. 01)	
V_4O_{10} ($^1T_2$)	1.40		−0.37	−0.68					

previous work,[18] at low values of the electron localization function η, a unique domain is found, which splits into several domains containing fewer attractors than the parent one upon increase of η. Ordering the values of η at which separations occur, it is possible to build tree-diagrams reflecting the hierarchy of basins. The partition or bifurcation of the core and valence domains is called the core/valence bifurcation, and it can occur in two different ways: either the core irreducible domains split before the valence ones or a valence division in two or more domains takes place before the core/valence separation. The first process characterizes ions or molecules, whereas the latter is typical for independent fragments in interaction.

The localization domain reduction tree-diagrams of the most stable cationic and neutral systems are given as Supporting Information 4S. As a general rule, the core/valence bifurcation takes place before the splitting into "child" domains at values of about $\eta = 0.12$. Nevertheless, systems containing O_2 units show a division of the parent domain into two parts before the core/valence bifurcation appears, i.e., $\eta = 0.09$ for the first splitting and 0.12 for the core/valence division, as for $V_2O_6^+$ (^{4}A) and $V_2O_7^+$ (^{2}A). The detailed analysis of these diagrams show the structure of the clusters, which coincides with the most favorable dissociation channels.

$V_2O_2^+$ presents the core/valence bifurcation at $\eta = 0.12$. At a value of 0.20 the V1 vanadium core basin splits leaving a VO_2 unit. This unit's bifurcation pattern follows the one corresponding to VO_2 and, according to this analysis, $V_2O_2^+$ model B can be considered as a V^+ and a VO_2 unit. Neutral V_2O_2 is a symmetric system and splitting of the valence domain into V and VO_2 units occurs without previous V−O basins separation. A valence vanadium basin for each vanadium atom appears at ELF values about 0.36, assigned to the presence of 3d electrons.

$V_2O_3^+$ shows the core/valence bifurcation at $\eta = 0.13$, while at 0.20 a division of the domain in VO and VO_2 units occurs. The VO unit splits at 0.40 like the VO^+ (3Σ) system; the VO_2 unit splits at 0.30 following the pattern of the neutral VO_2 cluster. From these results we deduce that the $V_2O_3^+$ system would be composed of a VO^+ and a VO_2 fragment. V2 presents a splitting into valence vanadium basin at further values of ELF, because it has electrons in the 3d orbital. Neutral system presents separation into a VO and a VO_2 domains at $\eta = 0.22$. Valence vanadium basins appear at ELF values of 0.37 and 0.38.

$V_2O_4^+$ presents a splitting into a VO and a VO_3 unit at 0.19. The VO part splits following the pattern of the VO^+ system. However, the VO_3 fragment does not present a V(O,O) basin as for the cluster VO_3, probably because of the interaction with the vanadium atom V2. No vanadium valence basins are present, since the formal oxidation states for V1 and V2 are (+5) and V(+4), respectively, and there are no 3d electrons. Neutral cluster presents a separation of the valence ring oxygens basins at 0.23. At a value of $\eta = 0.37$ terminal oxygen valence basins appear together with the vanadium core basins. This bifurcation pattern is different from the cationic one, and a separation into two symmetric VO−O units would be a better representation for this system. This fact is in agreement with the calculated dissociation channels, which render $VO^+ + VO_3$ for the cation and 2 VO_2 units for the neutral systems. No valence vanadium basins appear since no 3d electrons are present (vanadium oxidation states are (+4, +5) and (+4, +4) respectively).

$V_2O_5^+$ presents a bifurcation diagram similar to the $V_2O_4^+$ system, splitting into VO_2^+ and VO_3 fragments at $\eta = 0.30$ and 0.31, respectively. V_2O_5 follows the trend of the V_2O_4 and the valence domain separates into VO_2 and VO_3 domains at an ELF value of 0.17. Further splitting occurs for both fragments at 0.39 and 0.31, respectively. These bifurcation diagrams are in agreement with the dissociation channel results.

For $V_2O_6^+$, a valence domain separation leading to an O_2 unit and a $V_2O_4^+$ unit appears at an ELF value of 0.20. The $V_2O_4^+$ fragment undergoes VO^+ and VO_3 as with the $V_2O_4^+$ cluster. $V_2O_6^+$ (^{4}A) shows a separation of the parent domain into a O_2 and a $V_2O_4^+$ domain before the valence/core bifurcation, indicating that this cluster is composed of two independent parts, O_2 and $V_2O_4^+$. For these two systems, a disynaptic valence attractor between two oxygen atoms is present at $\eta \approx 0.70$, pointing out the covalent bond between O5 and O6. The neutral system does not present O−O bonds, but two terminal O (−1) atoms. The lone-pair basins for these oxygens appear in the bifurcation tree-diagram at $\eta = 0.30$, while the corresponding O (−2) appear at values of 0.37.

$V_2O_7^+$ shows a bifurcation diagram similar to that of the $V_2O_6^+$ clusters. The core/valence bifurcation takes place after the division of the parent domain into O_2 and $V_2O_5^+$, therefore it is possible to consider this system as two independent units weakly interacting. The O_2 fragment follows the bifurcation pattern of the O_2 molecule, while the cation diagram is analogous to that of the $V_2O_5^+$. For the neutral system the core/

TABLE 4: Valence Basin Population for the Most Stable Clusters (in electron)

	C(V1)	C(V2)	C(O1)	C(O2)	C(O3)	C(O4)	C(O5)	C(O6)	C(O7)	V(O ,O)	V(O1)	V(O2)	V(O3)	V(O4)	V(O5)	V(O6)	V(O7)
$V_2O_2^+$ ($^2A'$)[a]	21. 05	20. 54	2.1 7	2.1 2							7.1 4	7.1 0					
V_2O_2($^3A_{1'}$) [a]	20. 99	20. 58	2.1 5	2.1 3							7.2 3	7.2 4					
$V_2O_3^+$ ($^2A'$) [a]	20. 52	20. 73	2.1 2	2.1 3	2.1 2						6.8 1	7.2 4 [b]	7.2 9 [b]				
V_2O_3 ($^3A'$)	20. 44	20. 73	2.1 2	2.1 3	2.1 2						7.0 2	7.2 9	7.2 6				
$V_2O_4^+$ ($^2A'$)	20. 25	20. 52	2.1 6	2.1 2	2.1 2	2.1 1					6.7 5	7.0 8	7.1 0	6.7 7			
V_2O_4($^3B_2$)	20. 25	20. 53	2.1 2	2.1 2	2.1 2	2.1 1					6.7 5	7.0 9	7.0 9	6.7 7			
$V_2O_5^+$ ($^2A''$)	20. 26	20. 15	2.1 1	2.1 3	2.1 3	2.1 1	2.1 1				6.7 3	7.0 5	7.0 3	6.4 8	6.67		
V_2O_5($^1A'$)	20. 23	20. 16	2.1 7	2.1 4	2.1 5	2.1 2	2.1 2				6.8 7	7.1 0	7.0 9	6.9 1	6.92		
$V_2O_6^+$ (^2A)	20. 32	20. 25	2.1 2	2.1 3	2.1 1	2.1 2	2.1 8	2.1 2		1.00	6.7 5	7.0 5	7.1 0	6.7 4	5.73	5.30	
$V_2O_6^+$ (^4A)	20. 50	20. 23	2.1 0	2.1 1	2.0 9	2.1 4	2.1 9	2.1 1		1.04	6.7 9	7.1 5	7.1 1	6.7 5	5.52	5.16	
V_2O_6(^2A)	20. 12	20. 12	2.1 2	2.1 2	2.1 2	2.1 1	2.1 2	2.1 1			6.7 7	7.1 5	7.1 5	6.5 9	6.77	6.59	
$V_2O_7^+$ ($^2A''$)	20. 22	20. 15	2.1 6	2.1 3	2.1 3	2.1 1	2.1 1	2.1 1	2.1 1	1.28	6.7 5	7.0 4	7.0 6	6.6 9	6.48	5.34	5.10
V_2O_7 (^3A)	20. 15	20. 11	2.1 5	2.1 3	2.1 3	2.0 8	2.0 6	2.1 0	2.1 0	0.92	6.8 6	7.1 4	7.1 1	6.8 2	6.65	5.74	5.73
$V_3O_6^+$ ($^3A''$)	20. 20	20. 49	2.1 2	2.1 3	2.1 4	2.1 2					6.7 6	7.1 7	6.8 0	7.2 6			
V_3O_6($^4A'$) [a]	20. 37	20. 36	2.1 3	2.1 3	2.1 2	2.1 2					6.9 2	7.3 0	6.9 3	7.3 2			
V_3O_7+ (^1E)	20. 14		2.1 2	2.1 2							6.7 2	7.1 1	7.1 7				
V_3O_7($^2A''$)	20. 42	20. 12	2.0 5	2.1 6	2.1 3	2.1 3					6.9 7	7.1 5	6.8 7	7.1 1	7.30		
V_4O_{10} ($^1T_2$)	20. 08		2.1 0	2.1 2							6.8 5	7.1 8					
O_2 ($^3\Sigma_g^-$)			2.1 3	2.1 3						1.10	5.3 1	5.3 1					

[a] Present a valence vanadium basin (see text). [b] See text.

valence bifurcation occurs at $\eta = 0.15$, and at 0.25 two different domains appear, corresponding to a O_2 unit and a V_2O_5 which behave as the V_2O_5 in the excited ($^3A'$) electronic state (not shown).

The $V_3O_6^+$ cluster presents a separation into a $V_2O_3^+$ and a VO_3 domain at $\eta = 0.17$, these fragments follow the bifurcation diagrams of their corresponding species. The neutral system shows a separation of the ring oxygens at 0.22, and at 0.39 V2 core basins and O3 valence basins appear. At 0.41 the fragment VO corresponding to V1 and O1 appear. Vanadium valence basins are present, despite the formal absence of 3d electrons.

For $V_3O_7^+$, the valence basin of the central oxygen appears at 0.21, followed by the ring and terminal oxygens' valence basins. The neutral cluster bifurcation diagram shows a division of the valence domain into a VO unit and a V_2O_6.

The V_4O_{10} bifurcation diagram is characteristic of a molecule. Core/valence bifurcation occurs at $\eta = 0.10$. At ELF values of 0.24 ring oxygen valence basin separates, and at 0.40 the terminal oxygens' valence basins appear together with the vanadium core basins.

To sum up, the majority of the clusters present the core/valence bifurcation before the splitting of the parent domain into smaller domains, this is related to the most stable fragmentation patterns. However, for $V_2O_6^+$ (^4A) and $V_2O_7^+$ (^2A) the core/valence bifurcation takes place after it. Except for these two systems, $V_xO_y^+$ and V_xO_y ($x = 1-4$, $y = 2-10$) can be considered as stable "molecules" although they can be understood as an arrangement of smaller units. Systems containing O_2 units present three different bifurcation diagrams: the O_2 weakly interacting with the rest of the cluster is characterized by the core/valence bifurcation before the splitting into these units; superoxo O_2^- unit presents a splitting into the corresponding domains at ELF values of 0.20; finally, peroxo O_2^{2-} domain splits at slightly larger ELF values ($\eta \approx 0.25$). The ring oxygens' valence basins always appear before the terminal oxygens' basins, at $\eta \approx 0.25$ and 0.40, respectively. Regarding terminal oxygens, O (-2) valence basins appear at ELF values slightly larger than O (-1), i.e., 0.35 and 0.40, respectively. For the small clusters, V_2O_2 and V_2O_3, valence vanadium basins appear at $\eta \approx 0.36$, probably resulting from the presence of 3d electrons.

Basin populations for the most stable compounds have also been calculated and are reported in Table 4. Valence $V(O_i)$ basins are represented as unique basins for simplicity, although they are initially classified as disynaptic V(V,O) basins. Valence vanadium basin populations are not included in the Table but are discussed below.

$V_2O_2^+$ presents two nonequivalent vanadium atoms and oxygen atoms from the point of view of the ELF population analysis. No disynaptic attractors are found between vanadium core and oxygen core basins, so an ionic bond can be considered. Valence oxygen basins $V(O_i)$ present a population of 7.14 and 7.10 electrons and are symmetrically nonequivalent. Vanadium atoms present core populations of 20.54 and 21.05 for V1 and V2. The contribution of the V1 atom to the nonequivalent oxygen valence basins is 0.14 and 0.11 electrons, while the contribution of V2 to the same basins is 0.16 and 0.17 electrons. Relative covariances between V1 and the oxygens are in the range of 0.30, while for V2 they raise to 0.50, indicating more delocalization of the electronic density for the latter. From these results one can say that the interaction of V2 with oxygen atoms has a more covalent character than that corresponding to V1. Similar populations are found for the neutral cluster. The contribution of V1 and V2 to the valence equivalent oxygen basins are about 0.10 and 0.20 electrons, respectively. It is interesting to note that vanadium valence basins are present for both cationic and neutral systems. The population of these basins is 0.60−0.28 electrons for V1−V2 in $V_2O_2^+$ and 1.02−0.63 electrons for V1−V2 in V_2O_2. This fact indicates that a) there are 3d electrons in vanadium atoms, since their oxidation state is low (+2), (+3), and b) the addition of an electron to the cationic system occurs in the 3d orbitals of the vanadium V2, i.e., the isolated vanadium atom, not in the VO_2 fragment.

The $V_2O_3^+$ basins' population is quite similar to that of the previous system $V_2O_2^+$, regarding vanadium core basin population. A terminal oxygen is now present and the corresponding valence basin possesses 6.81 electrons. Regarding the ring oxygen population, it is slightly larger than the corresponding $V_2O_2^+$ ones. This can be attributed to computational problems, and the valence vanadium basin population has been included into the valence ring oxygens basins. Neutral system shows similar results with respect to V_2O_2, although this compound does not present a valence vanadium basin: the terminal oxygen valence basin has smaller population than the ring one.

$V_2O_4^+$ presents nonequivalent vanadium atoms, and terminal oxygens as well as ring oxygens. Vanadium V2 presents the highest core basin population; terminal oxygens show valence basins population of 6.75 electrons, while ring oxygen valence

basins' population is slightly larger, 7.10 electrons. No disynaptic attractors are present between vanadium and oxygen atoms, and therefore the bond is mostly ionic. The contribution of the vanadium atoms to the valence basins of terminal oxygen atoms is 0.30 electrons, with a covariance higher than 0.90. These values are abnormally large for pure ionic bonds, and a significant covalent character is found for vanadium-terminal oxygen bonds. The situation for ring oxygens is slightly different: a contribution of vanadium atoms V1 and V2 of approximately 0.18 and 0.13 electrons respectively is found, and covariances of 0.50 and 0.30 indicate a less-effective electronic delocalization between these basins in comparison with the terminal oxygens. Thus, a population analysis of the ELF density permits us to distinguish between terminal and ring oxygens. Moreover, the values presented above lead us to consider a stronger vanadium-ring oxygen interaction for V1 than for V2, so this $V_2O_4^+$ system can be thought to be composed of a VO and a VO_3 fragment.

The $V_2O_5^+$ description is similar to the previous $V_2O_4^+$ one. In this case, an oxygen with an oxidation state of (−1) is present, characterized by a valence basin population, 0.19 electrons lower than that corresponding to a O(−2). For the neutral system no differences in valence terminal populations are found.

$V_2O_6^+$ (^{2}A) presents a disynaptic attractor between O5 and O6 with a population of 1.00 and a covariance of 0.71, clearly indicating the presence of a covalent bond. As reference, the O_2 molecule presents a V(O,O) population of 1.10 electrons. The oxygen atoms in this unit show an asymmetric distribution of valence basins population: 5.73 electrons for the oxygen next to the cation and 5.30 electrons for the other one, while the O_2 molecule lone-pair basin population is 5.31.[18] A noticeable charge transfer of 0.35 electrons occurs from the $V_2O_4^+$ unit to the O_2 fragment. The contribution of V1 to V(O5) is small, and an ionic bond is expected. For $V_2O_6^+$ in the quadruplet electronic state, a disynaptic basin appears again between the two oxygens in the O_2 unit, with a population of 1.04 electrons and a fluctuation of 0.71. The population of the lone pairs for these oxygen atoms is 5.52 for the atom next to the cation, and 5.16 being the average approximately equal to the O_2 molecule. The interaction of this unit with the cation yields a small charge transfer of 0.04 electrons. Thus, a different interaction of the O_2 unit is observed: a stronger interaction for the doublet, involving a charge transfer of 0.35 electrons to the O_2 unit, and a weak interaction involving no significant charge transfer. It is possible to assign the former to a superoxo O_2^- species and the latter to a weak molecular interaction, in agreement with geometrical and frequency data. V_2O_6 most stable arrangement does not involve disynaptic valence basins. However three different oxygens are observed: a terminal O(−2) oxygen, having a valence basin population of 6.78 electrons; a terminal O(−1) oxygen, with a population of 6.59 electrons and ring oxygens, and a population of 7.15 electrons.

$V_2O_7^+$ basin population analysis is analogous to that of the $V_2O_6^+$ (^{4}A). V_2O_7 presents a different sort of interaction between O_2 and V_2O_5 fragments. The two oxygens of the O_2 unit are equivalent and possess a valence basin population of 5.74 electrons, larger than that corresponding to the O_2 molecule and the previously analyzed O_2^-. The population of the disynaptic valence basin between O6 and O7 is 0.92, with a fluctuation of 0.76. A charge transfer of 0.65 electrons from the V_2O_5 to the O_2 unit is observed. We assign this interaction to the peroxo O_2^{2-} unit.

$V_3O_6^+$ presents terminal oxygens with valence oxygen basin populations around 6.80 electrons, and ring oxygen atoms with populations about 7.20. The most charged basins correspond to the oxygens in the V_2O_3 unit described above. The neutral clusters present slightly larger values for oxygen valence basins; vanadium V2 valence basins possess a population of 0.14 electrons each, and a fluctuation of 0.93, indicating a large delocalization.

$V_3O_7^+$ is described as the $V_3O_6^+$ cluster, having a central oxygen valence basin of 7.17 electrons. This basin has a contribution of the vanadium atoms of 0.10 electrons each and a covariance of 0.25, because this atom is mostly ionically bonded to the three vanadium atoms. The neutral cluster presents the largest oxygen valence basin population, 7.30 electrons. The same trend is observed for V_4O_{10}.

To sum up, the absence of valence basin attractors between vanadium and oxygen atoms indicates a mostly ionic bond. Nevertheless, the contribution of the vanadium atoms to the valence basins of terminal oxygen atoms is about 0.30 electrons, with a covariance higher than 0.90. These values are abnormally large for pure ionic bonds, and a significant covalent character is found for vanadium-terminal oxygen bonds. The situation for ring oxygens is slightly different: a contribution of vanadium atoms of approximately 0.15 electrons is found, and covariances of 0.40 indicate a less-effective electronic delocalization between these basins in comparison with the terminal oxygens. It is possible that the distinction between terminal oxygens, i.e., O(−2) and O(−1) oxidation states in terms of basins population, is that the former is about 0.3 electrons more than the latter. The covariance is also slightly higher for O (−2). Systems containing O_2 units can be analyzed in terms of valence oxygen basin population: O_2 weakly interacting shows no charge transfer from the cationic unit to the O_2 fragment; superoxo O_2^- unit presents a noticeable charge transfer of 0.35 electrons to the O_2 valence basins, as well as an asymmetric population distribution in these basins; peroxo O_2^{2-} unit shows a charge transfer of 0.65 electrons. The characteristic disynaptic V(O,O) basin presents a population of approximately one electron and a fluctuation about 0.90, indicating a high delocalization between the two oxygen nuclei.

4. Conclusions

In the present work, the geometrical and electronic structure of $V_xO_y^+$ and V_xO_y ($x = 2-4$, $y = 2-10$) clusters at different electronic states have been investigated using a combination of DFT and Hartree−Fock calculations. A topological study based on the ELF analysis is carried out in order to understand the nature of bonding. The results of this work can be summarized as follows: i) The most stable structure for each cluster is: $V_2O_2^+$ (^{2}A′), $V_2O_3^+$ (^{2}A′) ≈ (^{4}A″), $V_2O_4^+$ (^{2}A′), $V_2O_5^+$ (^{2}A″), $V_2O_6^+$ (^{2}A), $V_2O_7^+$ (^{2}A″) ≈ (^{4}A″), $V_3O_6^+$ (^{3}A″), $V_3O_7^+$ (^{1}E), V_2O_2 (^{3}A$_1$), V_2O_3 (^{3}A′), V_2O_4 (^{3}A″), V_2O_5 (^{1}A′), V_2O_6 (^{3}A), V_2O_7 (^{3}A), V_3O_6 (^{4}A′), V_3O_7 (^{2}A″), V_4O_{10} (^{1}T$_2$). ii) Geometrical parameters and IR frequency data for cationic and neutral V_xO_y ($x = 2-4$, $y = 2-10$) species in different electronic states have been reported, and the structures obtained for the different clusters are in agreement with available experimental data. iii) The calculated geometrical parameters for the ground electronic states of V_2O_4, V_2O_5, V_2O_6, V_2O_7 (^{3}A), V_3O_8, and V_4O_{10} are similar to recently reported values of Vyboishchikov and Sauer. iv) Three different values of V−O distances are found: short (1.55 Å), intermediate (1.70−1.80 Å), and large (2.00 Å). These values can be associated to strong (terminal) and weak interactions involving O(−2) and O(−1) oxidation states, respectively. v) Structures possessing a V_2O_2 ring ($V_2O_2^+$ (^{2}A′), $V_2O_3^+$ (^{2}A′) ≈ (^{4}A″), $V_2O_4^+$ (^{2}A′), $V_2O_5^+$ (^{2}A″), $V_2O_6^+$ (^{2}A), $V_2O_7^+$ (^{2}A″),

V_2O_2 ($^3A_1$), V_2O_3 ($^3A'$), V_2O_4 ($^3A''$), V_2O_5 ($^1A'$), V_2O_6 (^3A), and V_2O_7 (^3A)) present higher stability than their corresponding linear or branched arrangements. vi) The results of the energy for the dissociation channels suggest that VO^+ ($^3\Sigma$), VO ($^4\Sigma$), VO_2 ($^2A_1$), VO_3 ($^2A'$), and O_2 ($^3\Sigma_g^-$), constitute the building blocks for the more complex clusters moieties. vii) Cationic and neutral V_2O_4, V_2O_5, V_3O_6, V_3O_7, and V_4O_{10} constitute stable species, in accord with experimental data. viii) From the ELF analysis, the vanadium oxygen bond can be considered as mostly ionic, according to the absence of a disynaptic basin between these two atoms. However, a partial covalent character is found as the basin population analysis points out. ix) For $V_2O_6^+$(^2A), $V_2O_7^+$ ($^2A''$), and V_2O_7 (^3A) clusters, a disynaptic basin is found between two oxygen atoms, indicating the presence of a O_2 unit. ix) According to the bifurcation diagrams, $V_2O_2^+$ ($^2A'$) is composed of V^+ and VO_2 units, while V_2O_2 ($^3A_1$) shows a V and a VO_2 part. $V_2O_3^+$ ($^2A'$) can be described in terms of VO^+ and VO_2 units, and V_2O_3 ($^3A'$) is formed by VO and VO_2. The $V_2O_4^+$ ($^2A'$) cluster presents VO^+ and VO_3 fragments while V_2O_4 ($^3A''$) is composed of two VO_2 units. $V_2O_5^+$ ($^2A''$) can be described as VO_2^+ and VO_3 while V_2O_5 ($^1A'$) is formed by VO_2 and VO_3 fragments. The $V_2O_6^+$ (^2A) cluster presents a core/valence bifurcation into O_2 and $V_2O_4^+$, while V_2O_6 (^3A) shows two terminal O(−1) atoms bonded to a V_2O_4 fragment. $V_2O_7^+$ ($^2A''$) can be considered as independent $V_2O_5^+$ and O_2 weakly interacting, whereas V_2O_7 (^3A) presents V_2O_5 and O_2 nonindependent fragments. $V_3O_6^+$ ($^3A''$) is formed by $V_2O_3^+$ and VO_3 fragments, while V_3O_6 ($^4A'$) does present the typical diagram of a molecule. $V_3O_7^+$ (^1E) is composed of V_3O_6 and O units, while V_3O_7 ($^2A''$) presents VO^+ and V_2O_6 fragments. V_4O_{10} ($^1T_2$) can be considered as a stable molecule. x) Different interactions between O_2 and fragments have been characterized: a molecular O_2 is present for $V_2O_7^+$ ($^2A''$); a superoxo O_2^- interaction is found for $V_2O_6^+$ (^2A); a peroxo O_2^{2-} unit is present for V_2O_7 ($^3A''$).

Acknowledgment. This work is supported by DGICYT (proyecto PB96-0795-C02-02). M.C. is grateful to Conselleria de Cultura, Educació i Ciència (Generalitat Valenciana) for a doctoral fellowship. Computer facilities of the Servei d'Informàtica (Universitat Jaume I) are acknowledged.

Supporting Information Available: Dissociation channels (eV) for the most stable models **1S**; Vibrational frequency values (cm^{-1}) and the corresponding intensities in parentheses for $V_2O_y^+$ and V_2O_y clusters ($y = 2-7$) **2S**; Vibrational frequency values (cm^{-1}) and the corresponding intensities in parentheses for $V_{3-4}O_y^+$ and $V_{3-4}O_y$ clusters ($y = 6-10$) **3S**. Localization domain reduction tree diagrams for the most stable cations and neutral clusters **4S**. This material is available free of charge via the Internet at http://pubs.acs.org.

References and Notes

(1) Cox, P. A. *Transition Metal Oxides. An Introduction to Their Electronic Structure and Properties;* Clarendon Press: Oxford, 1992.
(2) Rao, C. N. R.; Raveau, B. *Transition metal oxides*; VCH Publishers: New York, 1995.
(3) Berkowitz, A. E. In *Magnetic Properties of Fine Particles;* Dormann. J., Fiorani, D., Eds.; North-Holland: Amsterdam, 1992.
(4) Busca, G.; Lietti, L.; Ramis, G.; Berti, F. *Appl. Catal. B: Environmental* **1998**, *18*, 1.
(5) Yamanaka, I.; Morimoto, K.; Soma, M.; Otsuka, K. *J. Mol. Catal. A* **1998**, *133*, 251.
(6) Viparelli, P.; Ciambelli, P.; Lisi, L.; Ruoppolo, G.; Russo, G.; Volta, J. C. *Appl. Catal. A* **1999**, *184*, 291.
(7) Gao, X.; Wachs, E. *J. Phys. Chem. B* **2000**, *104*, 1261.
(8) Bell, R. C.; Zemski, K. A.; Kerns, K. P.; Deng, H. T.; Castleman, A. W., Jr. *J. Phys. Chem.* **1998**, *102*, 1733.
(9) Bell, R. C.; Zemski, K. A.; Castleman, A. W., Jr. *J. Phys. Chem. A* **1998**, *102*, 8293.
(10) Bell, R. C.; Zemski, K. A.; Castleman, A. W., Jr. *J. Phys. Chem. A* **1999**, *103*, 2292.
(11) Bell, R. C.; Zemski, K. A.; Castleman, A. W., Jr. *J. Phys. Chem. A* **1999**, *103*, 1585.
(12) Foltin, M.; Stueber, G. J.; Bernstein, E. R. *J. Chem. Phys.* **1999**, *111*, 9577.
(13) Martins, J. B. L.; Longo, E.; Andr'es, J. *Int. J. Quantum Chem.* **1993**, *27*, 643.
(14) Martins, J. B. L.; Andr'es, J.; Longo, E.; Taft, C. A. *J. Mol. Struct. (THEOCHEM)* **1995**, *330*, 301.
(15) Sambrano, J. R.; Andr'es, J.; Beltr'an, A.; Sensato, F.; Longo, E. *Chem. Phys. Lett.* **1998**, *287*, 620.
(16) Beltr'an, A.; Andr'es, J.; Noury, S.; Silvi, B. *J. Phys. Chem. A* **1999**, *103*, 3078.
(17) Calatayud, M.; Beltr'an, A.; Andr'es, J.; Silvi, B. *Chem. Phys. Lett.* **2001**, *333*, 493.
(18) Calatayud, M.; Andr'es, J.; Beltr'an, A.; Silvi, B. *Theor. Chem. Acc.* **2001**, *105*, 299.
(19) Vyboischchikov, S. F.; Sauer, J. *J. Phys. Chem. A* **2000**, *104*, 10913.
(20) Frisch, M. J.; Trucks, G. W.; Schlegel, H. B.; Gill, P. M. W.; Johnson, B. G.; Robb, M. A.; Cheeseman, J. R.; Keith, T.; Peterson, G. A.; Montgomery, J. A.; Raghavachari, K.; Al-Laham, M. A.; Zakrzewski, V. G.; Ortiz, J. V.; Foresman, J. B.; Cioslowski, J.; Stefanov, B. B.; Nanayakkara, A.; Challacombe, M.; Peng, C. Y.; Ayala, P. Y.; Chen, W.; Wong, M. W.; Andres, J. L.; Replogle, E. S.; Gomperts, R.; Martin, R. L.; Fox, D. J.; Binkley, J. S.; Defrees, D. J.; Baker, J.; Stewart, J. P.; Head-Gordon, M.; Gonzalez, C.; Pople, J. A. *GAUSSIAN94, Revision B1*; Gaussian, Inc.: Pittsburgh PA, 1995.
(21) Rassolov, V. A.; Pople, J. A.; Ratner, M. A.; Windus, T. L. *J. Phys. Chem.* **1998**, *109*, 1223.
(22) Becke, A. D. *J. Chem. Phys.* **1993**, *98*, 5648.
(23) Lee, C.; Yang, R. G.; Parr, R. G. *Phys. Rev. B* **1988**, *37*, 785.
(24) Veliah, S.; Xiang, K.-h.; Pandey, R.; Recio, J. M.; Newsam, J. M. *J. Phys. Chem. B* **1998**, *102*, 1126.
(25) Gutsev, G. L.; Rao, B. K.; Jena, P.; Wang, X.-B.; Wang, L.-S. *Chem. Phys. Lett.* **1999**, *312*, 598.
(26) Nayak, S. K.; Jena, P. *J. Am. Chem. Soc.* **1999**, *121*, 644.
(27) Gutsev, G. L.; Khanna, S. N.; Rao, B. K.; Jena, P. *J. Phys. Chem. A* **1999**, *103*, 5812.
(28) Reddy, B. V.; Jena, P. *Chem. Phys. Lett.* **1998**, *288*, 253.
(29) Gutsev, G. L.; Rao, B. K.; Jena, P. *J. Phys. Chem. A* **2000**, *104*, 11961.
(30) Han, J.-G. *Chem. Phys. Lett.* **2000**, *324*, 143.
(31) Becke, A. D.; Edgecombe, K. E. *J. Chem. Phys.* **1990**, *92*, 5397.
(32) Savin, A.; Nesper, R.; Wengert, S.; Fässler, T. *Angew. Chem., Int. Ed. Engl.* **1997**, *36*, 1809.
(33) Krokidis, X.; Noury, S.; Silvi, B. *J. Phys. Chem.* **1997**, *101*, 7277.
(34) Chesnut, D. B. *J. Phys. Chem. A* **2000**, *104*, 11644.
(35) Fuster, F.; Sevin, A.; Silvi, B. *J. Phys. Chem. A* **2000**, *104*.
(36) Silvi, B.; Gatti, C. *J. Phys. Chem. A* **2000**, *104*, 947.
(37) Savin, A.; Jepsen, O.; Flad, J.; Andersen, O. K.; Preuss, H.; von Schnering, H. G. *Angew. Chem.* **1992**, *31*, 187.
(38) Savin, A.; Silvi, B.; Colonna, F. *Can. J. Chem.* **1996**, *74*, 1088.
(39) Berski, S.; Silvi, B.; Lundell, J.; Noury, S.; Latajka, Z. In *New Trends in Quantum Systems in Chemistry and Physics*; Maruani, J., Ed.; Kluwer Academic Publishers: 2001; Vol. 1; p 259.
(40) Marx, D.; Savin, A. *Angew. Chem., Int. Ed. Engl.* **1997**, *36*, 2077.
(41) Llusar, R.; Beltran, A.; Andres, J.; Silvi, B.; Savin, A. *J. Phys. Chem.* **1995**, *99*, 12483.
(42) Noury, S.; Krokidis, X.; Fuster, F.; Silvi, B. Topmod Package Paris, 1997.
(43) Noury, S.; Krokidis, X.; Fuster, F.; Silvi, B. *Comput. Chem.* **1999**, *23*, 597.
(44) Silvi, B.; Savin, A.; Kempf, J. Y.; von Schnering, G. *Bull. Polish Acad. Chem.* **1994**, *42*, 413.
(45) Haber, J.; Witko, M.; Tokarz, R. *Appl. Catal., A* **1997**, *157*, 3.
(46) Bytheway, I.; Wong, M. W. *Chem. Phys. Lett.* **1998**, *282*, 219.